THE ZONE OF METAL PHASE CONSUMPTION IN GAS-METAL REACTIONS[1]

ANDREW DRAVNIEKS AND HUGH J. McDONALD

Corrosion Research Laboratory, Illinois Institute of Technology, Chicago, Illinois

ABSTRACT

It is shown by an analysis of the scale growth process that the scale of even approximately uniform composition formed in the reaction between gas and metal must consist of at least two layers. One layer is formed by the outward migration of metal ions and electrons through the scale; the other forms under the scale in the zone of consumption of the metal phase. Both layers form under completely different conditions. The inner layer is vital for the maintenance of metal transport to the bulk of the scale and grows at a gas pressure of the order of the dissociation pressure of the scale substance. It is demonstrated that the inner layer will develop cavities. A third layer may be formed in some secondary process, for example, that of recrystallization. It is therefore evident that the concept of a uniform process of scale growth is an oversimplification and fundamentally incorrect. This conclusion is supported by an investigation on copper iodide scale. The protective film formation on aluminum and the accelerated growth of oxide films on metals at the beginning of oxidation are explained on the basis of the considerations presented above.

INTRODUCTION

In this paper an attempt is made to outline some particular phases of scale formation in gas-metal reactions. Because of our present highly inadequate knowledge of diffusion rates in solids, mutual solubilities of solids and gases in solids and surface tensions in solid-solid interfaces, the treatment must necessarily be in part of a speculative character. In order to render the presentation more fluent, an oxygen-metal system will be employed as the model for the various considerations, although the same reasoning applies to all gas-metal reactions where scale is formed.

According to the generally prevailing views, the oxidation of metals at elevated temperatures in an oxygen-containing atmosphere has usually been described as film or scale formation going on mainly by the mechanism of diffusion of metal through the scale toward the oxide-gas interface. This mechanism was shown to function in the case of oxidation of iron investigated by Pfeil (1). The same mechanism was found to hold in several other gas-metal reactions investigated by Wagner and his coworkers (2, 3, 4), with a further refinement of treating the diffusion of metal as separate diffusion of cations and electrons. The differences in ionic and electronic conductivities of oxide enabled Mott (5) to provide an explanation for the protective film formation on aluminum. A recent investigation by Dravnieks and McDonald (6), who measured the electropotential differences set up in growing scales, gave full support to the electrochemical

[1] Manuscript received June 6, 1948. This paper prepared for delivery before the New York Meeting, October 13 to 16, 1948.

theory of scale formation. It may be remarked that the mode of growth will be different in the case of anionically conducting scales.

The diffusion of oxygen through the oxide toward the metal was assumed to exist to some extent by most investigators but was disregarded because obviously it did not play any considerable role in determining the rate of reaction. The diffusion of oxygen was demonstrated, for example, by Rhines and his coworkers (7, 8, 9, 10, 11) in the scale formation on alloys.

Closer analysis of the scale formation process as made in the present paper shows that the region between the scale and the metal is the stage of rather complicated events. The only investigators who have paid attention to this region so far are Pfeil (1) and Smirnov (12). Pfeil described the morphological properties of this region, consisting of loose oxide columns. Smirnov considered the space geometrical aspects as correlated to the volume changes and ratios of the diffusion constants of oxygen and metal through the scale formed at slightly elevated temperatures. He was able to develop a formal mathematical expression which could explain different shapes of time vs. scale formation curves.

The zone of metal phase consumption

Let us visualize the following experiment (Fig.1): a specimen of ideally smooth pure metal is brought into intimate contact with a thin and equally ideally smooth layer of oxide. The oxygen gas phase is then placed on the other side of the oxide layer. The experiment being ideal, no oxygen will be able to pass to the surface of the metal except by way of diffusion through the oxide lattice. If the diffusion of metal, presumably in the form of cations and electrons, now starts through the oxide, metal atoms leave the metal phase and travel toward the oxide-gas interface; that is, the metal phase is consumed.

Obviously, holes will remain in the metal-oxide interface and the areas of direct contact between the metal and oxide will decrease and the boundary of the metal will retreat. It is, therefore, clear that the usually visualized concept of the scale as an ideally uniform phase with an essentially constant gradient of chemical potential across it cannot be valid. In fact, the region in the space between the locus of the former metal surface and the boundary of the retreating metal phase must be the site of some processes which maintain material contact between the scale and metal. This region may be denoted as the zone of metal phase consumption.

Two fundamental layers of scale

If the above-mentioned hypothetical experiment is continued, it can easily be shown that the concept of a one-layer scale is fundamentally wrong and by virtue of growth the scale must consist of at least two layers. Indeed, assume that the ratio

$$R = \frac{\text{Volume of compact oxide which is formed from 1 mole of metal}}{\text{Volume of 1 mole of metal}}$$

(Pilling-Bedworth ratio, modified in expression) is larger than unity, so that a continuous scale can be formed. If, now, a certain volume of scale is newly formed on the outside of the oxide layer, it must mean that an equivalent but smaller volume of metal phase has been consumed. The

oxide phase will be separated from the metal phase by a certain space. It is evident that this space cannot exist unfilled. This space can either disappear by sinking of the scale toward the metal or must become filled with the oxide crystals. The first case is unlikely except if the oxide substance is very weak mechanically so that the oxide columns or layers formed eventually can collapse under the external pressure. However, this possibility must be kept in mind if oxidation at very high pressures is considered.

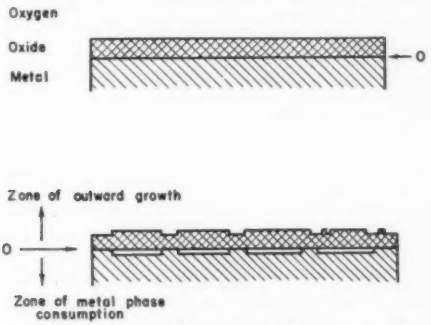

FIG. 1. A situation may be imagined like that in Fig. 1 where an ideal oxide layer is placed in ideal contact with a metal surface. Obviously if, as assumed, metal atoms or ions can move by diffusion through the oxide, the next situation will immediately arise as shown on the bottom part of the figure. Here, several metal atoms have left their positions in the lattice of the metal phase, escaped into the lattice of oxide and some of them have arrived on the surface of the scale. New oxide lattice cells have been formed.

It may be deduced that the scale must consist fundamentally of two layers located in two zones. The first zone may be designated as that of outward growth. The second phase, under the scale, is the zone of metal phase consumption. This is the locus below the initial metal surface.

It is seen that in order to grow, the scale must grow on both sides. The purpose of growth on the inside is the maintenance of contact with the metal phase so that the metal atoms can be supplied to the bulk of the scale and to the outside growth zone. The extension of the scale on both sides proceeds under entirely different conditions. On the outside of the scale there is a comparatively plentiful supply of oxygen from the gas phase. On the inside, the partial pressure of oxygen is very low, of the order of the dissociation pressure of the scale. Consequently, there is good reason to expect that crystal aggregates will acquire different morphological forms in different zones.

Under usual oxidation conditions, the second situation is the most likely one, namely where the space which was previously occupied by metal phase is filled with crystal aggregates or columns of oxide.

It follows that the oxide layer which was placed on the metal cannot continue to grow in only one direction—outward. It must also grow inward, toward the retreating metal phase. The crystal aggregates or columns must follow the boundary of the metal phase and act as conduits which will deliver metal atoms to the bulk of the scale. Therefore, these crystal columns must be in a state of continual growth.

To form these columns, oxygen and metal are the necessary components. Two processes can be devised to supply the necessary oxygen. First, the oxygen atoms can arrive by way of diffusion through the scale. Second, the

oxide scale may dissociate, oxygen being freed into the hole and the liberated metal atom escaping toward the outer surface of the scale.

Consequently, the conditions of formation of oxide lattice cells are completely different if both sides of the scale are compared. The formation of oxide on the outside of the scale goes on under a plentiful supply of oxygen, provided that the external pressure is not too low. On the contrary, the formation of oxide in the zone of metal consumption usually occurs at a very low pressure of oxygen which is determined by the phase equilibrium between the gas phase in the hole and the two solid phases present. Now, it must be emphasized that neither the oxide nor metal phases are pure, that is, of unique and uniform composition. The former is usually a solid solution of either vacant sites or interstitial ions in the oxide. The metal phase is frequently a solid solution of oxygen in metal. Therefore, the oxygen pressure is not uniquely defined by the temperature of the system but depends also on the concentration of oxygen in both phases. This concentration can vary in a certain range and will generally depend on the concentration of oxygen in the external gas and condition of scale growth.

It may be concluded that the scale will consist principally of two fundamental layers formed by processes operating under different conditions; therefore, both layers will ultimately be different in their texture.

The sequence of processes in the metal consumption zone

Let us analyze the processes responsible for the formation of holes and oxide lattice cells in the zone of metal consumption.

The first layer of metal adjacent to the oxide layer will disappear easily, going into the lattice of the oxide. An empty space of unicellular thickness will be formed and will spread laterally (Fig. 1, bottom). Such space cannot exist, as an extended flat crystal surface is not possible from the standpoint of the molecular kinetic theory. The Maxwell-Boltzmann distribution law requires that such a flat surface, if created, immediately degenerate into one with holes and atoms placed on the surface of the average level line (Fig . 2). The number of holes and atoms placed on the surface will be determined by the usual exponential factor containing the term $-\frac{\Delta\epsilon}{kT}$ in the exponent, where ϵ accounts for the excess energy per atom if transported from the outside layer of surface, leaving a hole, to the position sitting on the surface. For example, Volmer (13) calculated that the number of holes and outstanding atoms on the flat surface of an atomic crystal is of the order 10^9–10^{10} per square centimeter. The total number of atoms in the surface of this size is of the order of 10^{14}. It must be remembered that the situation is a dynamic one and the surface is involved in a continuous process of placing some atoms in outstanding positions and filling the holes in the inverse process.

This implies that the disappearance of the layer of unicellular thickness does not necessarily mean the complete discontinuance of contact between the metal and oxide. Scattered points all over the metal and oxide surfaces facing each other will come into contact and the over-all situation will resemble that of two hilly surfaces placed in contact.

Now another process will enter the scene. The chemical potential of

phases of small dimensions and, consequently, larger curvature is larger than that of larger dimensions and smaller curvature. Therefore, the protruding surface sections of smaller dimensions will tend to disappear preferentially and the zones of contact between metal and the bulk of the oxide will concentrate on columns of larger dimensions which will support the scale. Thus it is seen that the primarily formed space of unicellular thickness will develop into a cavity of multicellular and eventually microscopic dimensions, containing a gas phase.

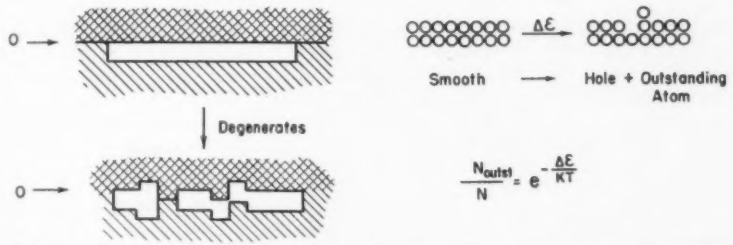

FIG. 2. Fig. 2 shows the hypothetical situation which would arise if at some moment the scale and metal are separated by a space of monatomic thickness. Such ideally smooth surfaces are unstable from the standpoint of the Maxwell-Boltzmann distribution law. If the energy difference in going from the smooth surface to the surface with a hole and an outstanding atom is denoted by $\Delta\epsilon$, then the fraction of outstanding atoms will be, by the distribution law, equal to

$$e^{-\frac{\Delta\epsilon}{KT}}$$

where K is Boltzmann's constant. Calculation for an average atomic lattice shows that there would usually be 10^{10} such defects per square centimeter of surface.

It should be remembered that the situation will be dynamic. New holes and outstanding atoms will arise continually and the existing defects will disappear. This consideration implies that the first hypothetical situation cannot exist and the smooth surfaces will degenerate. The metal and oxide phases will come into occasional contact here and there, outstanding metal atoms will escape into the oxide scale, and the space of monatomic thickness will continue to grow to form a cavity of two-, three-, and four-atomic thicknesses. In this way a cavity of appreciable dimensions should develop from an initially small empty space.

The gas phase in the cavity will consist of the vapor of the metal, the vapor of the oxide, and oxygen at very low pressure. The first two components can usually be neglected and will be disregarded in the considerations below. The pressure of oxygen is of the order of the dissociation pressure of the oxide. At low temperatures, this pressure can become so low that the concentration of oxygen in the cavity will be insufficient to support any reasonable rate of exchange of oxygen between the phases forming the cavity. At the usual high temperatures employed in the investigations of scale growth, the pressures of oxygen are of the order of 10^{-5} to 10^{-25} atmospheres.

As soon as cavities of larger extent are developed, the supplying of metal to the bulk of the scale is slowed down. The chemical potential of metal in the inside surface of the bulk scale is lowered and that of oxygen raised.

The conditions may be understood on the basis of Fig. 3. Here the black discs represent the chemical potential of oxygen in the surface of the scale facing the cavity. The oxygen can leave the oxide only if a place is available where the chemical potential of oxygen is lower. Oxygen in the gas phase of the cavity will be present at about the same chemical potential as long as it is not decreased by the dynamics of processes taking place around the cavity. Oxygen will also cover the metal and oxide column

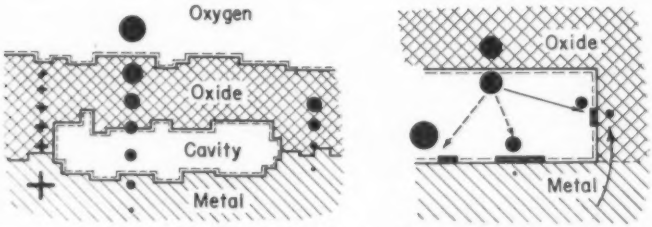

FIG. 3. Now the situation is shown in Fig. 3. Here the black discs symbolize the chemical potential of oxygen in the gas, scale, cavity, and in dissolved form in the metal phase. The plus signs are the chemical potentials of metal in the metal and scale. It is assumed that oxygen in the oxide is practically immobile so that only metal can migrate through the oxide along the gradient of chemical potential. However, oxygen can cross the cavity going from the place of higher chemical potential to that of lower potential. If an oxygen atom leaves the oxide lattice in the process of dissociation of an oxide cell, the freed metal atom is available for diffusion outward. This is another process by which a cavity can expand or move in the space.

The right part of the figure symbolizes the possible paths of migration of oxygen. In order to produce a new cell of oxide, oxygen must meet metal atoms. This can happen in various places around the cavity, for instance on the surface of the metal. However, the first oxide cell will be a plateau of small dimensions. The chemical potential of oxygen in such a phase of small dimensions is appreciably high as indicated by a large black disc. Such occasionally precipitated oxide cells will, therefore, tend to dissociate immediately. If, by some statistical distribution, a larger plateau were suddenly formed of a size larger than some critical value, the chemical potential would drop so that the growth of the oxide phase will be continued.

There is still another place where metal atoms are available. In the oxide column are some metal atoms in the process of migration outward. If oxygen combines with these metal atoms, new cells of oxide phase will form on the base of the oxide already present. In such cases, it may be shown from considerations of surface energies that the critical size which must be reached in order to grow is much smaller because of similar lattices. The new cells will probably be still more stable if deposited at the base of the column.

It may be concluded that, under the conditions described in this discussion, the most probable process is the thickening of oxide columns and spreading of column bases.

surfaces with an incompletely saturated unimolecular adsorbed layer, being present in the adsorbed layer with approximately the same chemical potential as in the solid below the layer.

The formation of oxide by passing of the adsorbed layer into a new layer of oxide cells is tied in with the formation of new surfaces, so that an excess of work is necessary to create these surfaces. This requirement necessitates that a certain finite excess of chemical potential of oxygen is necessary in order to start transport of oxygen from the bulk of the scale.

In general, if a plateau of oxide cells has to be set up on some carrier surface, the additional work contributing to the chemical potential of

oxygen in the plateau is equal to the difference between the work spent in creating new surfaces and that gained in the disappearance of the surface area of the carrier covered by the plateau. The surface areas to be created are: the area of the sides of the plateau, the top area of the plateau adjoining the gas phase, and the base area of the plateau. The base area of the plateau is the oxide/carrier interface. There are two kinds of carriers available, namely, the metal surface, and the side surface of the column. The column contains excess metal which is in the process of diffusion toward the bulk of the scale, so that the chemical potential of oxygen is decreasing in the direction of the metal surface.

Generally, the additional work to be done in the formation of the plateau will depend on the magnitude of the surface energy of the plateau/carrier interface and this work is smaller if the lattices of the plateau and carrier are similar. Unfortunately the present knowledge of surface energies of solid/solid interfaces is inadequate and does not allow any consistent quantitative treatment of the process. Qualitative consideration, how-

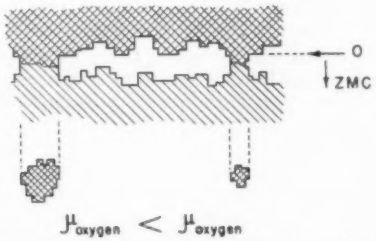

FIG. 4. Fig. 4 shows the simple process of oxygen exchange between the oxide columns of different sizes.

The chemical potential μ of oxygen in the smaller column is larger than that in the thicker one. Therefore, the thicker columns will grow and the thinner columns will generally tend to disappear. By the same process, the protruding parts of the oxide phase will also tend to disappear.

ever, shows that a smaller excess of chemical potential will be required to build up a new plateau of the oxide somewhere at the side of the oxide column near the metal surface.

An allowance must be made for the cases where, because of the statistical distribution fluctuations of energy and oxygen atoms, a spontaneously formed small oxide plateau on the metal surface might exceed some critical size with a subsequent drop of chemical potential below the value prevalent for the cavity. Then additional columns could grow from this nucleus. This probability will depend to a large extent on the actual values and ratios of the constants involved.

From the above considerations it is seen that the extension of the oxide lattice into the zone of metal phase consumption will proceed most probably by way of thickening of the oxide columns (Fig. 4).

Supplying oxygen to the metal consumption zone

To extend the scale lattice into the metal consumption zone, it is necessary to supply oxygen to the space between the scale and metal.

Obviously, three processes can be offered to carry on the supplying of

oxygen, provided that the metal itself was oxygen-free at the commencement of the scale growth. First, oxygen can be supplied through cracks. Second, oxygen can be freed into the space between the scale and metal by dissociation of the scale at the inner scale surface. Third, oxygen can arrive at the zone of metal phase consumption by regular ionic or atomic diffusion through the lattice of the scale. Also, there may be simultaneous functioning of two, or all three, of these processes. So far, the experimental evidence is too meager to decide in favor of a particular process. The first process functioning alone seems to be unlikely, as the scale, if growing by metal diffusion through the scale, will tend to seal cracks immediately. The second process allows an approximate calculation. Many metal oxides possess, at temperatures where the scale growth is moderately rapid, low dissociation pressures. If molecular velocities and gas pressures as low as 10^{-15} to 10^{-30} atm. are employed for the purpose of calculation, the transport of oxygen across the cavity, e.g., 10 Angstroms in thickness, comes out to be much too slow to provide for any scale growth in the metal consumption zone. However, there is an uncertainty as to the velocity with which the oxygen atoms or ions leave the surface of the oxide during dissociation. It is quite reasonable to expect that the actual concentration of oxygen atoms and especially ions very close to the surface of the dissociating oxide is much larger than at appreciable distances from the surface; the whole situation is similar to electron cloud formation in thermoelectronic emission. Therefore, if very close to the oxide surface, another metal surface is placed which can catch oxygen, the actual concentration of oxygen in the space between them may be much larger than judged by dissociation pressures obtained from equilibrium studies. Consequently, the mechanism of scale dissociation cannot be discarded simply because the known dissociation pressures lead to an evidently incorrect order of magnitude for the oxygen exchange rate.

The supply of oxygen by regular diffusion through the scale lattice seems to be a feasible process and, in fact, some workers, e.g., Valensi (17), favor the view that the diffusion of oxygen through scales, for instance through nickel oxide, is an important rate-determining process in scale growth.

It seems reasonable to assume that, whatever may be the mechanism of supplying oxygen to the metal consumption zone, it may in some cases become the rate-determining process. More experimental evidence is necessary to detect particular cases where it is actually rate-determining.

Formation of secondary layers

It has been shown that even if the formation of layers differing in the valency of the metal component is excluded and the metal is present throughout the scale in prevalently the same valency state (disregarding the difference in valency caused by disorder conditions in the lattice), there must exist at least two layers of different textures. Further, a third layer could be formed in some secondary process.

One such secondary process would be possible if the oxygen could be supplied into the cavity not only by diffusion through the scale but also by dissociation of the oxide. Then there will develop a new layer in the space where the compact scale was formerly present but has dissociated,

leaving merely crystalline aggregates necessary to carry on the transport of matter from the metal phase to the scale.

Another process which may be responsible for the third layer formation is recrystallization (Fig. 5). There is good reason to believe that while oxidation is continued and the upper part of the metal consumption zone filled with crystalline aggregates becomes more amd more distant from the metal phase, the crystals in that part tend to go over into more stable larger

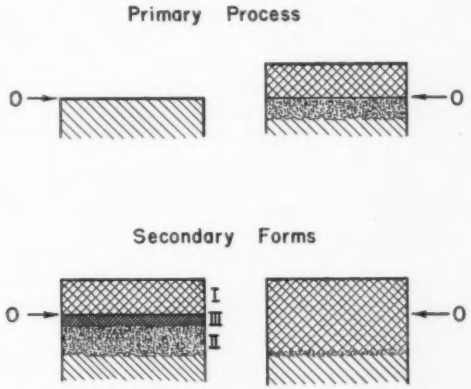

FIG. 5. The collective effect of the described processes is shown in Fig. 5. The metal phase reacts with the gas and forms a compact outside layer and a porous inside layer. The porous layer is formed in the zone of metal phase consumption. The porosity is caused by processes already discussed. It may be mentioned that Pfeil, in 1929, in his investigation of the scaling of iron observed such a porous layer between the locus of the initial metal surface and the remaining metal phase. The oxide columns extend toward the retreating metal phase and act as conduits which function by delivering metal atoms to the bulk of the scale.

Simultaneously with these complex primary processes, different secondary processes may proceed. One of the most important secondary processes is the recrystallization of the virgin porous layer, resulting in more stable large crystals being formed. This causes the appearance of an intermediate third layer.

If the recrystallization is very fast, the third layer may be relatively thick and the virgin porous layer may shrink to a thin zone adjacent to the metal phase surface. In such a case, a pseudo-uniform scale is observed as seen in the lower right-hand corner. This situation is frequently encountered because scaling reactions are usually investigated at temperatures where rates of reaction are of considerable magnitude. Consequently, the mobility of the reactants is appreciable which, in turn, favors recrystallization.

crystals and approach; in appearance, the crystals formed by the scale growth outward. The process of recrystallization is favored by the increased mobility of oxide lattice components, as the usual experiments on the oxygen-metal reactions are performed at temperatures where scale growth is easily observed and therefore the mobility is naturally high.

It may be concluded that formation of a third layer in scale growth, as a consequence of secondary processes, is very probable. In cases where the recrystallization is comparatively rapid, the third layer may be indistinguishable from that formed on the outside of the scale, and the scale

will consists of two distinct layers: a thin one representing the zone of metal phase consumption in its virgin state, and a thick one which is formed in two different ways, by scale growth outward and by secondary recrystallization of the virgin layer formed in the zone of metal phase consumption. This case can be observed, for example, in oxide scales on copper.

Experimental evidence

In the oxidation of metals such as iron, copper, nickel, cobalt, etc., several layers corresponding to different valency states are usually formed and the general picture is obscure. However, Pfeil (1) in his investigation of the oxidation of iron observed a layer of oxide columns extended like stalagmites in the space between the compact scale and the metal phase. This observation is in complete agreement with the considerations presented in this paper.

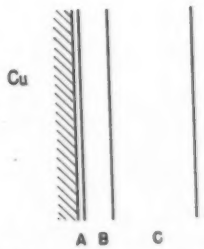

FIG. 6. Layers in the scale of cuprous iodide on copper

The authors investigated the formation of cuprous iodide on the surface of electrolytic copper at 360°C. in an atmosphere of nitrogen and iodine. The deductions made for the formation of oxide scales apply as well to other gas-metal systems, and cuprous iodide is very convenient because of its rapid and uniform formation. Cuprous iodide is the only layer substance formed in this reaction. This is an advantage as conditions are more clear-cut than in multi-layer oxide scales on metals. The outward growth of the scale was easily detected by placing zirconium oxide and platinum particles on the surface before the experiment. The particles were found embedded in the scale after the experiment.

The cross-sections of specimens made immediately after removal from the oven revealed that the scale consists of three layers, completely different in appearance, as shown in Fig. 6.

The inner layer A was very thin and consisted of loose yellowish powder. The intermediate layer B was a grey powder, not as finely crystalline as A. The layer, C, was thick, coarsely crystalline and compact, dark and semi-transparent.

X-ray graphs taken of the three layers failed to show any significant difference in the lattice constants. All three layers were pure cuprous iodide phases. This result serves as evidence that the three layers were formed in different processes under different conditions. The difference in colors may be ascribed to the differences in the size of crystals and to the

different degree of deviation from stoichiometric composition due to disorder in the lattice. Left in air for several days, the sections acquired a uniform white color. However, the difference in the crystal sizes and textures is sufficient proof for the different conditions of formation.

As the particles of zirconium oxide mentioned above were usually found partly in the coarse crystalline A layer and partly in the outer boundary of layer B, the following interpretation may be feasible. Layer A is formed by growth outward, the layer C is the virgin iodide phase formed in the zone of metal consumption, and the layer B is the product of recrystallization of the virgin iodide phase.

Formation of protective scales

It seems possible that in certain cases the range of the values of chemical potentials of oxygen in oxide may be narrow and, on the other hand, the additional work of building up new oxide plateaus is considerable. Then, the thickening of the columns in the metal consumption zone will be considerably hindered, especially when the dissociation pressure of oxide is very low. Under these conditions the first layers of the scale will still form fast due to the fact that the metal can be supplied to the scale all over the area by statistically distributed high points in the flat exposed metal surface. The columns will form in places where impurities are present. But there would be practically no thickening of the remaining columns and the delivery of metal through columns of small cross-section will lead to a practical cessation of scale growth. Those conditions may account for the protective non-growing films on aluminum, providing a concurrent explanation to that proposed by Mott (5). It is probable that both mechanisms work hand in hand, Mott's mechanism being responsible for the non-diffusion through columns. If the apparent thickness of protective alumina film as determined by weight increase is of the order of 50 Å, the true thickness, taking into account the surface roughness factor of 2–3, will be of the order of 15–25 Å corresponding to a layer of 3–4 lattice cells in thickness. This is the right order of magnitude of thickness to which any thin film of oxide can grow without employing the mechanism of column thickening. The probable impurities may be inclusions of aluminum oxide.

"Linear" growth of thin films

Evans (14) put forward considerations explaining rapid linear growth of oxide film in the early stage of film formation. Gulbransen (15, 16) observed experimentally the accelerated growth of oxide films at the beginning of the oxidation. Because of experimental uncertainties, it is not possible to determine the exact law of growth at this stage and it may only be stated that the growth is faster than that corresponding to the usual parabolic growth.

This accelerated growth is easy to understand if the same considerations as employed in the case of protective layer formation are employed. The parabolic growth corresponds to the diffusion rates through the simultaneously and proportionally growing two fundamental layers. The initial growth rate corresponds to the diffusion through the outer scale layer under conditions when the cavities and columns in the zone of metal consumption just start to develop.

Correlation between diffusion rate and rate of growth

Considering that the scale consists of at least two layers, it must be concluded that any apparent diffusion rate, if calculated from the rate of scale formation, cannot be directly correlated to the diffusion rate through the lattice of the oxide. The causes which can be held responsible for the eventual deviations are of a two-fold nature.

First, the metal ions and electrons on their way to the outer surface scale have to pass through two layers of different crystal size and different thickness. The outer layer is solid and compact, the inner one is formed by loose columns of undefined total cross-section per unit area of specimen.

Second, not all the mass of the consumed metal phase has to travel the same distance to the outside of the scale. Part of the metal is used up already under the scale for the purpose of building up the transportation system functioning between the metal phase and the bulk of the scale.

The influence of these two effects is to some extent opposed. Also the increase of the thickness of both scale layers is about proportional. Therefore, the fundamental structural differences in the scale are hidden behind usually nicely shaped parabolic growth curves. However, the conformity to the parabolic law does not lie in the nature of the scale growth, and every condition disturbing the proportionality of layers or exchange of oxygen in cavities will cause the rate to deviate from the parabolic curve.

One of the factors which is likely to disturb the normal development of the scale layers is frequently met in investigations of metals of technical purity. This factor is the gases dissolved or occluded in the metal. Even if present in small amounts, they will be liberated into cavities and interfere with the exchange of oxygen between the places of different chemical potential. However, the effect cannot be rate-limiting directly, as can be judged by the experiments of Pfeil (1) who found that the exchange of oxygen between two scales heated in nitrogen goes on at a considerable rate. More likely, the presence of foreign gas will influence the forms of crystal columns and act indirectly.

SUMMARY

1. Even in the case when a scale grows by outward diffusion of metal or metal ions, the scale must also grow on the other side, toward the metal. The name *zone of metal phase consumption* is proposed for this second zone of growth.

2. The conditions of scale growth on both sides of the scale are dissimilar and, consequently, the structure of the scale tends to be different in the two layers.

3. The processes of cavity and column formation and exchange of oxygen in the zone of metal phase consumption are outlined.

4. Dissociation and, especially, recrystallization are responsible for the frequent occurrence of a third layer formation as a consequence of secondary processes.

5. Additional evidence for the outlined mechanism is provided by an X-ray investigation of cuprous iodide scale.

6. Protective film formation and pseudo-linear growth of thin films are discussed in the light of considerations presented in the paper.

7. The difficulties involved in treatment of scales as uniform layers are emphasized.

ACKNOWLEDGMENT

The research work reported in this paper was done under contract with the U. S. Navy, Office of Naval Research. The authors wish to acknowledge the suggestions made during the early part of this work by Dr. James T. Waber, now of the Los Alamos Scientific Laboratories. The X-ray patterns were obtained through the courtesy of Dr. E. J. Bicek.

Any discussion of this paper will appear in the discussion section of Volume 94 of the Transactions of the Society.

REFERENCES

1. L. B. Pfeil, *J. Iron Steel Inst.*, **64**, 504 (1929).
2. C. Wagner, *Z. physik. Chem.*, **B 21**, 25 (1933).
3. ———, *Ibid.*, **B 32**, 447 (1936).
4. C. Wagner and K. Grünewald, *Ibid.*, **B 40**, 455 (1938).
5. N. F. Mott, *Trans. Faraday Soc.*, **35**, 1175 (1939), **43**, 429 (1947).
6. A. Dravnieks and H. J. McDonald, *J. Electrochem. Soc.*, **93**, No. 5, 177 (1948).
7. F. N. Rhines, *Trans. Am. Inst. Min. Met. Eng.*, **137**, 246 (1940).
8. F. N. Rhines, W. A. Johnson, and W. A. Anderson, *Ibid.*, **147**, 205 (1942).
9. F. N. Rhines and A. H. Grobe, *Ibid.*, **147**, 318 (1942).
10. F. N. Rhines and B. S. Nelson, *Am. Inst. Min. Met. Eng.* T.P. 1617 (1943).
11. F. N. Rhines, *Ibid.* T.P. 1645 (1943).
12. A. A. Smirnov, in V. I. Arkarov "Oxidation of Metals," Sverdlovsk-Moskwa (1945).
13. M. Volmer, "Kinetic der Phasenbildung," Verl. Steinkopff, Dresden (1939).
14. U. R. Evans, discussion on H. A. Miley's paper, *Trans. Electrochem. Soc.*, **81**, 407 (1942).
15. E. A. Gulbransen, *Ibid.*, **82**, 375 (1942).
16. ———, *Ibid.*, **83**, 301 (1943).
17. G. Valensi, "Pittsburgh International Conference on Surface Reactions," p. 156, Corrosion Pub. Co., Pittsburgh, Pa. (1948). Also private communication

A NEW ELECTROLYTIC CELL FOR MAGNESIUM AND CHLORINE PRODUCTION[1]

B. G. HUNT

The Consolidated Mining and Smelting Company of Canada, Limited, Trail, British Columbia, Canada

ABSTRACT

A new type of electrolytic cell has been developed for the production of magnesium and chlorine from molten magnesium chloride electrolyte. The design features close spacing of electrodes, elimination of the usual refractory partition between anode and cathode, and a separate metal well. The major objectives—simple and compact design, low power consumption, and direct casting of metal from the cell—have been realized with the added advantage of high chlorine gas strength. Construction and operation of a cell rated at 10,000 amperes are described in detail and the design of a 30,000 ampere cell is discussed briefly.

An extensive research program on various processes for the production of magnesium, conducted by The Consolidated Mining and Smelting Company of Canada, Limited, Trail, British Columbia, showed that the most satisfactory process under local conditions would involve electrolysis of molten anhydrous magnesium chloride. This paper describes a new type of cell developed for this purpose.

The raw materials available to the Company and the conditions obtaining

[1] Manuscript received June 14, 1948. This paper prepared for delivery before the New York Meeting, October 13 to 16, 1948.

at its operations at Trail indicated that the best process to be adopted should include calcination of magnesite to form magnesium oxide, chlorination of the oxide to produce magnesium chloride, and subsequent electrolysis of the chloride to yield metallic magnesium. In this process, the two major problems to be solved were the development of a suitable method for producing the magnesium chloride, and the design of an improved cell for reducing the chloride to metal. The first problem was satisfactorily solved by the Consolidated Mining and Smelting Company; the successful solution of the second problem was a result of a joint research program carried out with the Mathieson Alkali Works, Inc. (now Mathieson Chemical Corporation).

Two types of magnesium cell which have been used extensively on this continent are the M. E. L. cell, of Magnesium Elektron Limited, and the Dow cell, of Dow Chemical Company. The M. E. L. cell operates on anhydrous magnesium chloride feed; the Dow cell operates on hydrous magnesium chloride feed. This difference in feed partly explains the difference in chlorine concentrations of the gas evolved from each of these cells; gas from the M. E. L. cell is relatively high in chlorine content whereas gas from the Dow cell is relatively low in chlorine content. Metal produced in the Dow cell may be cast into bars directly from the cell, but metal produced in the M. E. L. cell is further refined to remove electrolyte before casting into bars. Both types of cell make use of a partition or separator submerged slightly in the electrolyte between anode and cathode with the object of keeping the products of electrolysis separated and preventing their recombination.

In the work at Trail indications were obtained that, in magnesium chloride electrolyte, the rate of recombination of magnesium and chlorine liberated at the electrodes of a cell is not as high as had been commonly supposed, and that under certain conditions the usual partition disposed between anode and cathode would be unnecessary. With these considerations in mind, a project to design a satisfactory cell without the usual partition, but with reasonably high current efficiencies, was undertaken. The success of this project is recounted in this paper.

Several advantages would be obtained with a cell purposely designed without a partition. By eliminating the partition, the attendant problems of providing suitable construction material and satisfactory support for the partition would be eliminated.

Also, of course, without the partition the distance between anode and cathode could be reduced, thus lowering the ohmic resistance of the cell. The electrical efficiency of an electrolytic magnesium cell is measured by the power consumption per pound of magnesium produced, and power consumption is proportional directly to the cell voltage and inversely to the current efficiency. Although the current efficiency of a cell operating without the partition might be lowered because of recombination of magnesium and chlorine, it was hoped that the increase in power consumption caused by the lower current efficiency would be more than offset by the decrease in power consumption effected by the close spacing of the electrodes.

With this close electrode spacing, the cell could be smaller than the conventional type for an equivalent rate of metal production, leading to lower construction costs, smaller floor area requirements, and lower heat losses.

Furthermore, the gas lift action of the chlorine liberated in the relatively restricted space of the electrolysis zone would probably insure rapid circulation of the electrolyte with consequent uniform cell temperatures and electrolyte concentration.

According to the contemplated method of operation, a mixture of magnesium, electrolyte, and chlorine would be formed in the electrolysis zone and this mixture, it was assumed, would rise upward without excessive recombination of metal and chlorine.

The indicated advantages warranted investigation of the design and operation of a cell that would incorporate these various features. How this would be accomplished was not immediately apparent, but as the investigation proceeded, R. B. MacMullin, at that time one of Mathieson's engineers, and the author devised a suitable design and method of operation which, it was found, enabled these advantages to be obtained.[2] Several small test cells were constructed and operated with encouraging results. In the method of operation, the chlorine was first removed from the mixture of magnesium, electrolyte, and chlorine rising from the electrolysis zone, and the electrolyte and metal were passed together to a separate part of the cell in which the metal could accumulate and from which the electrolyte could return to the electrolysis zone. By this method of operation, the metal could be accumulated in amounts sufficient to allow casting marketable ingots directly from the cell.

In view of the promising results obtained with the small cells, a larger cell was built to operate with a current load of 10,000 amperes. This larger cell[3] was designed by the author and embodied improvements in internal construction but employed the same method of operation as the smaller cells, that is, firstly, the formation of a mixture of magnesium, electrolyte, and chlorine in the electrolysis zone, secondly, the separation of chlorine from the mixture of magnesium and electrolyte, thirdly, the separation of magnesium from the electrolyte, and finally, the return of the electrolyte to the electrolysis zone. This method of operation has been proved at Trail to be very satisfactory and has been employed throughout the work described in this paper.

The larger cell is illustrated in Fig. 1, and includes an electrolysis chamber containing four cylindrical steel cathodes with concentric graphite anodes. The electrode spacing is such that the annular cross-sectional area between anode and cathode is restricted in order to provide, with normal evolution of chlorine, a gas lift action in the electrolysis zone. A mixture of magnesium, electrolyte, and chlorine is formed in the electrolysis zone and the gas lift action causes this mixture to rise into the chlorine chamber, above the electrolysis chamber. In the chlorine chamber, the gas separates from the mixture and collects for withdrawal from the cell. The mixture of metal and electrolyte, free of chlorine, flows from the chlorine chamber through a submerged port into a separate metal well. The metal collects in the upper part of the well and the electrolyte returns from the bottom of the well to the bottom of the electrolysis chamber.

The diagram indicates that the electrolyte from the metal well passes through another compartment, a feed well, before returning to the electrolysis chamber. This separate feed well is not required when anhydrous

[2] B. G. Hunt and R. B. MacMullin, U. S. Pat. 2,393,686, 1946.
[3] B. G. Hunt, U. S. Pat. 2,393,685, 1946.

chloride is charged to the cell, as the anhydrous material can be fed into the metal well. Hydrous feed should not be added to the metal well, of course, as the water in the feed would react with the metal.

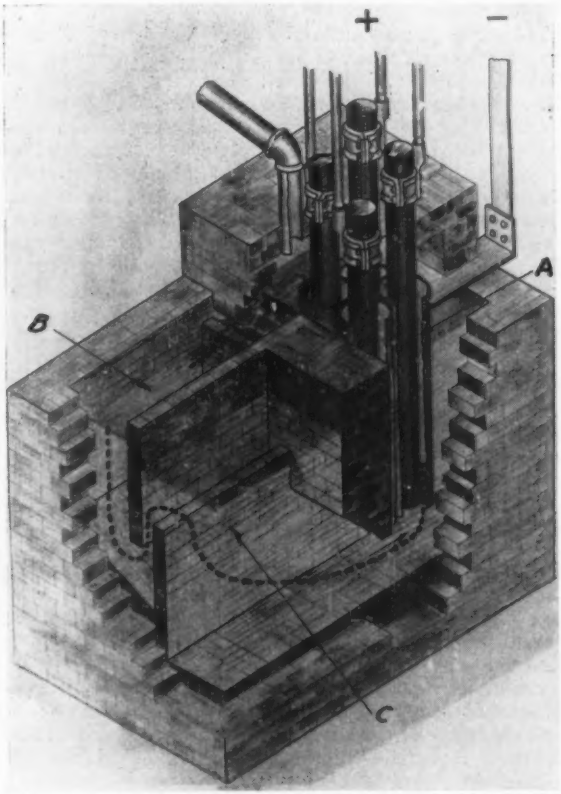

FIG. 1. Diagram showing cut-away view of experimental 10,000 ampere cell. A, electrolysis compartment; B, metal well; C, feed well.

CONSTRUCTION OF 10,000 AMPERE CELL

The container for the cell is a steel shell, with $\frac{1}{4}$-in. boiler plate for the sides and $\frac{3}{8}$-in. plate for the bottom. The outside dimensions are 7 ft. in length by 5 ft. $3\frac{1}{2}$ in. in width and 5 ft. 5 in. in height. The shell is lined with suitable refractory brick within which are the electrolysis and chlorine chambers and the metal and feed wells.

The cathode assembly consists of four vertical steel tubes welded to a horizontal plate which rests on the brick work and serves as a support for the cathode tubes and also as the cathode current lead-in.

In the final design, the cathode tubes were cast of 27 per cent chrome steel and were 9 in. inside diameter and 11 in. outside diameter. Graphite

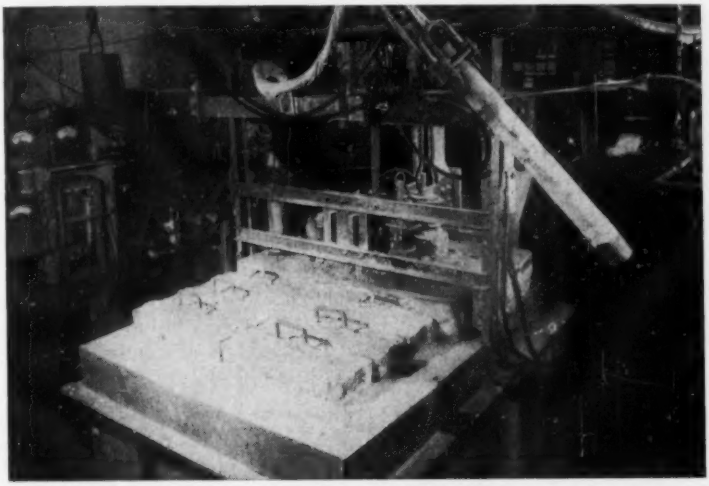

FIG. 2. General view of top of experimental 10,000 ampere cell. Covers on metal and feed wells, A.C. electrode out.

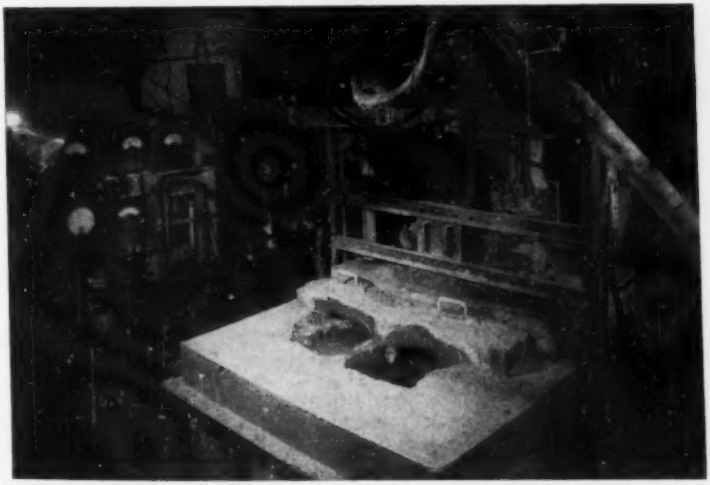

FIG. 3. General view of top of cell. Covers off wells and A.C. electrode out.

anodes of 7 in. diameter were centered in the cathode tubes, giving an anode to cathode distance of one inch.

The chlorine chamber has refractory lined sides and roof. The roof has four openings for anodes. There is also an off-take in the roof for the removal of chlorine. The inside dimensions of the chlorine chamber are 2 ft. 4¾ in. by 3 ft. in area by 9 in. deep. The free surface area of electrolyte in the chamber must be such that the chlorine gas rising as a froth from the electrolysis chamber may free itself from the electrolyte before the mixture of electrolyte and metal flows out through the passage to the metal well.

This passage is U-shaped and submerged below the liquid level. It has been found by experiment that the cross-sectional area of the passage should be approximately 2½ square inches for every 1,000 amperes of cell capacity. If the area is too small the passage will not allow sufficient flow of electrolyte to maintain circulation; the electrolyte level will rise in the chlorine chamber and magnesium will collect and be trapped in the chamber where it will be rechlorinated. Similarly, if the area is too large the electrolyte velocity becomes too low and magnesium tends to remain behind in the chamber. The passage is so designed that if the electrolyte circulation ceases temporarily a liquid seal remains, preventing either loss of chlorine if the gas system is under pressure or dilution of the chlorine with air if the gas system is under suction.

The metal collecting well is 14¾ in. by 13½ in. in area by 4 ft. 3 in. deep. The area must be sufficient to reduce the electrolyte velocity to a point where the metal readily separates from the electrolyte and accumulates at the surface. The depth should be enough to permit sufficient metal to accumulate for direct casting.

In this cell, a feed well was also incorporated. If the cell feed is to be only molten anhydrous magnesium chloride, the feed well is not necessary as this material can be charged into the metal well in the presence of metal. The feed well has a horizontal area of 20½ in. by 10½ in. and is 4 ft. 3 in. deep. A vertical slot in the refractory partition between the metal and feed wells directs the electrolyte from the bottom of the metal well to the top of the feed well. An opening from the feed well to the bottom of the electrolysis chamber allows the electrolyte to complete the circuit and also provides access to the bottom of the cell for removal of cell mud when necessary.

Provision for auxiliary heating by alternating current was made by inserting two 4 in. graphite electrodes in the feed well and connecting them to the secondary circuit of a low voltage transformer. Satisfactory heating was also obtained with only one auxiliary electrode by connecting one side of the secondary circuit to the cathode.

OPERATION OF 10,000 AMPERE CELL

When starting the cell, it is first filled with molten electrolyte of a conventional mixture of sodium chloride and anhydrous magnesium chloride. During filling, the auxiliary A.C. is used to maintain the salt in a fused state. When the electrolyte level is near the top of the cathodes, the direct current is applied. The chlorine evolved raises and starts the circulating action of the electrolyte almost immediately.

The electrolyte level is maintained by additions from time to time of magnesium chloride, preferably in the molten state as produced in a

chlorinator. However, as the volume occupied by the magnesium chloride in the electrolyte is partially replaced by the magnesium metal produced, most of the feed is added at the time the metal is removed. Only minor quantities of feed are required between metal removals.

The cell is designed to operate continuously at the full current rating of 10,000 amperes. Auxiliary A.C. heating is used to balance heat requirements owing to the low operating voltage (less than 5), particularly with new anodes. Cells are normally operated in series electrically; if one cell of the series overheats at 10,000 amperes, with fixed anodes, the temperature can be lowered to normal only by lowering the current input. This lowers the current to all cells of the series and may result in insufficient energy input to maintain the temperature of other cells. Lowering the current, of course, reduces the metal output proportionally and also reduces the rate of circulation of electrolyte due to evolution of less chlorine. As cell temperatures must be maintained, the power consumption per pound of metal produced increases. With these factors in mind, it was deemed advisable to design the cell to operate at full current capacity, starting with less voltage than necessary to fulfil all energy requirements and supplying the balance of the energy requirements by auxiliary A.C. heating.

A running-in period of several days is usually required before the cell reaches optimum operating conditions. Impurities such as iron have to be precipitated from the electrolyte and the cathode has to be conditioned. The action of cathode conditioning probably consists in the removal of scale and foreign matter and the exposure of a fresh metallic surface.

During the conditioning period, the magnesium metal is deposited in the form of small globules or prills. These prills do not adhere to the cathode long enough to build up to an appreciable size. Consequently, as the magnesium rises through the electrolytic zone in a finely divided state and in the presence of chlorine, there is some tendency toward rechlorination, thus lowering the net current efficiency. Once the electrolyte and cathode are conditioned, the magnesium apparently forms a film on the cathode, in effect a magnesium cathode, and the deposited magnesium rises through the electrolytic zone in contact with the cathode and finally breaks away at the top as large globules. It is thus cathodically protected while in the electrolytic zone.

These globules breaking away from the cathodes are flushed through the chlorine chamber out into the metal well. The metal is allowed to accumulate in the metal well and can be left in the cell for 24 hour periods without adverse effects, such as burning. The electrolyte level must be maintained, of course, to insure adequate circulation. While the metal is accumulating, only small amounts of feed are added, but this low rate of feed between dipping periods does not deplete the electrolyte of magnesium chloride to any serious degree. The overflow into the metal well imparts a stirring action to the metal bath. This tends to maintain a protective electrolyte film on the metal surface thus reducing the opportunity for oxidation by air. The metal well is covered, except during dipping operations, thus further protecting the metal from contact with air.

The metal is dipped with a teapot ladle from a deep layer, so that clean, electrolyte-free metal is obtained for casting directly into ingots or billets requiring no further refining before marketing. Casting directly from the

cell increases the over-all recovery of magnesium by eliminating the metallurgical loss in refining and also avoids the added cost of refining.

The usual formation of cell mud occurs, the amount depending largely on the quality of feed used. The mud is removed by dredging the bottom of the cell with a perforated ladle every second or third day.

The cell yields chlorine gas of the high strength of approximately 95 per cent. This gas requires little or no further treatment for use in the chlorinators producing the magnesium chloride for the cell, or in other processes.

CELL DATA

D.C. amperage—10,000
D.C. volts (average)—4.82
Anodes—graphite, 4 in number, 7 in. in diameter, 30 in. immersion, current density 3.79 amp./sq. in.
Cathodes—chrome steel, 4 in number, 11 in. outside diameter, 9 in. inside diameter, 30 in. immersion, current density 2.95 amp./sq. in.
Anode to cathode spacing—1 inch
Specific resistance of the electrolyte (calculated under operating conditions)—0.38 ohm per inch[3]

The specific resistance is considerably higher than that of a molten mixture of the same electrolyte under quiescent conditions. This is explained by the fact that the volume of the electrolytic zone is so restricted that it is largely occupied by the chlorine gas enveloping the anodes.

CELL PERFORMANCE

Magnesium produced per day, lb.			163.0
Current efficiency, per cent			68.0
Power consumption, KWH per lb. Mg	D.C.	7.09	
	A.C.	1.33	8.42
Magnesium recovery, per cent			95.3
Ratio of mud to metal produced			0.12:1.00
Average cell gas, chlorine per cent			95.0

The above data, obtained over an extended period, are representative when the cell was fed with the grade of feed prepared for the experiment. Despite the relatively small scale of operation, the power consumption compares favorably with that of conventional cells. It will be noted that the cell performance figures confirm the original assumption that power consumption could be reduced even with comparatively low current efficiencies. It is well known that cell performance is very sensitive to certain impurities in the feed, such as iron and boron, even if they are present in very small amounts. When special precautions were taken to purify the magnesium chloride before adding it to the cell, the current efficiency was raised to an average of 75.0 per cent and the power consumption lowered to 7.90 KWH per lb. of magnesium.

Throughout the experimental work conducted on the 10,000 ampere cell, a good deal of attention was paid to designing an efficient anode clamp. In cells of this type where the operating voltage is low, an appreciable part of the voltage (and consequently power consumption) may be lost in delivering the power from the bus bars to the electrolyte. An improved type of anode clamp[4] was developed which reduced the voltage drop across

[4] L. E. Leonard, U. S. Pat. 2,423,714, 1947.

it to a satisfactory minimum. The clamp delivers the current across a relatively small contact area under high mechanical pressure.

DESIGN OF 30,000 AMPERE CELL

On the basis of information obtained from the operation of the 10,000 ampere cells, a 30,000 ampere cell has been designed. So far there has been no opportunity to build and operate it.

The cell incorporates rectangular instead of cylindrical anodes and cathodes, thus using relatively less volume and conserving heat. As only anhydrous magnesium chloride feed was to be used, the feed well is eliminated, which further reduces the over-all size.

The rectangular anodes can be arranged more compactly than cylindrical anodes and give a smaller cell for the same current rating. They also simplify the problem of an efficient gas seal, thereby helping to reduce electrode consumption. In the experimental work on the 10,000 ampere cell, the anodes were subject to corrosion above the electrolyte where they were exposed at high temperatures for prolonged periods to a small concentration of air leaking into the chlorine chamber. In the 30,000 ampere cell, it is hoped that deterioration of the anodes will be eliminated except for electrolytic corrosion, which is low in cells operating with anhydrous magnesium chloride feed.

The outside dimensions of this cell are:

(a) Cell body—Length	9 ft.	11 in.
Width	7 ft.	3 in.
Height	4 ft.	9½ in.
(b) Anode top—Length	6 ft.	8½ in.
Width	5 ft.	9½ in.
Height		14½ in.

There are six rectangular graphite anodes each 30 in. by 4 in. in cross section and 60 in. in length. These are assembled into one unit using graphite spacers. The cathode assembly consists of a cast steel grid sufficiently rigid to avoid warping.

One compartment acts as both a metal and a feed well. Two electrodes in opposite sides of this compartment supply auxiliary A.C. heat when necessary for temperature control. The auxiliary A.C. power required is in the range of 40 to 50 KVA, and is applied at 1,400 to 1,600 amperes and 29 to 31 volts.

ANTICIPATED CELL PERFORMANCE

The following performance estimates are based on the data obtained from the operation of the 10,000 ampere cell.

Estimated Mg production, lb. per day			510.
Estimated current efficiency, per cent			71.
Estimated power consumption, KWH per lb. Mg	D.C.	5.9	
	A.C.	1.5	7.4
Estimated D.C. voltage			4.2
Estimated magnesium recovery per cent			95.0
Estimated anode gas per cent chlorine			95.0

ACKNOWLEDGMENT

The author wishes to acknowledge the cooperation and encouragement of R. B. MacMullin and W. C. Gardiner of Mathieson Chemical Corporation.

Permission to publish this paper has been given by the management of The Consolidated Mining and Smelting Company of Canada, Limited, and by the Mathieson Chemical Corporation.

Any discussion of this paper will appear in the discussion section of Volume 94 of the Transactions of the Society.

THE NATURE OF NEGATIVE IONS IN LIQUID HYDROCARBONS[1]

ANDREW GEMANT

Research Department, The Detroit Edison Company, Detroit, Michigan

ABSTRACT

This investigation was carried out with electrolytically conducting solutions in xylene and hydrocarbon oil, prepared by dissolving an organic amine, an aliphatic acid, and a phenolic compound in the hydrocarbon solvent. By means of potentiometric determinations, using silver electrodes coated with the silver salt of an aliphatic acid, it was shown that the negative ions in the solutions mentioned are essentially phenol-solvated anions of the aliphatic acid present. Corresponding determinations on oxidized oils indicate that the negative conducting particles in such oils might be fundamentally of the same type as those in the above mentioned solutions.

In a previous paper (1) the author has shown that electrolytically conducting solutions in hydrocarbons may be produced by dissolving an amine, an aliphatic acid, and a phenolic compound in the hydrocarbon as solvent. The positive ion may be pictured as the cation form of the amine, and the negative ion as the anion of the acid, to each of which a certain number of phenolic molecules are attached. In the present paper experimental proof is furnished concerning the nature of the negative ions in such solutions. This was done by means of potentiometric determinations. If the negative ions are anions of aliphatic acids, then an electrode capable of producing such ions should show a reversible potential difference against the solution, the emf having the sign and magnitude according to theoretical expectations. Silver was chosen as a suitable metal, the solid salt (2) in contact with it being the silver salt of an aliphatic acid.

The first experiments were carried out with xylene containing a small percentage of ethyl alcohol. In this case, the combined presence of an amine and an acid is sufficient to produce high conductivities. Tributylamine and myristic acid were chosen for these tests.

The cell for the emf measurements was similar to that used in previous work (3), consisting essentially of a U-tube, one half of which was used for a reference solution and the other half for any other solution, which will hereafter be called the variable solution. The reference solution mostly con-

[1] Manuscript received April 26, 1948. This paper prepared for delivery before the New York Meeting, October 13 to 16, 1948.

tained the same amine and acid as the variable solution but was kept at the relatively high conductivity level of 10^{-10} mho/cm. Silver myristate was prepared by precipitating the salt from silver nitrate and myristic acid solutions in ethyl alcohol containing 10 per cent water. Before each set of measurements was taken, the silver foil used for the two electrodes was cleaned with sandpaper and a small amount of the silver salt was smeared upon the surface.

Fig. 1 gives the potentials in mv. plotted against the logarithm of the conductivity ratio between the two solutions of the concentration cell.

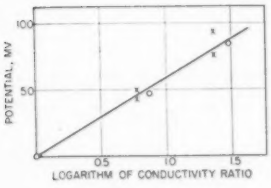

FIG. 1

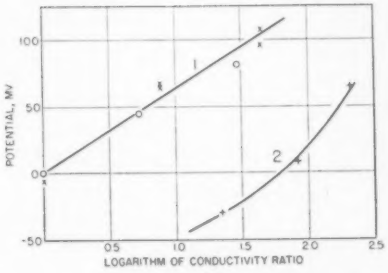

FIG. 2

FIG. 1. Potential difference vs. conductivity ratio for solutions of tributylamine and myristic acid in xylene, containing 3 (○) and 5 (×) per cent ethyl alcohol.

FIG. 2. Emf vs. conductivity ratio for solutions in xylene. Curve 1, no phenolic differential, ×—0.16 m. *o*-cresol, ○—0.12 m. α-naphthol; Curve 2, 0.12 m. phenolic differential.

The sign of the potential was taken as that of the electrode in the variable solution. As may be seen, the curve fulfills the well-known relation (3) for univalent ions

$$E = 118\, t_c \log_{10} (\sigma_r/\sigma) \qquad (1)$$

where the potential E is in mv., t_c is the transference number of the cation, σ_r and σ are the conductivities of the reference and the variable solution, respectively. As an approximation in this equation, the concentration of the anion is taken as being proportional to the electrical conductivity. From the slope of the curve, $t_c = 0.50$ is obtained. The same slope was obtained with solutions in pure ethyl alcohol. Since there can be little doubt that in these solutions the negative ions are myristate ions, these tests can be considered as proof that the silver silver-myristate electrode works according to theory, and that it may be used with confidence in unknown solutions.

Fig. 2 shows the results with xylene as solvent without the addition of ethyl alcohol. The solutions contained tributylamine, myristic acid, and a phenolic compound. The results (Curve 1) are similar to the previous ones.

The series, reproduced by Curve 2, refers to variable solutions containing no phenolic compound so that the phenolic differential was 0.12 mole since the reference solution for this set contained 0.12 mole/liter α-naphthol.

True concentration cells require the same solvent at both sides of the cell. The presence of a phenolic compound, whatever its mechanism, amounts to a change of the solvent inasmuch as the phenol solvatizes the ion. If a difference in phenolic concentration exists between two sides of a cell, its emf is not given by the free energy term shown by Equation (1). A second term arising from a difference in solvation energies must be added. An expression for this case was given in a previous paper (3); it was calculated on the basis of the difference in dielectric constants. This term is negative if the variable solution has a lower phenolic content than the reference solution, since a transfer of an anion from a higher to a lower phenolic concentration requires an increase of free energy. In keeping with this explanation, Curve 2 is shifted to lower-values, the shift being about 0.11 volt for a difference in α-naphthol concentration of 0.12 mole/-liter. The slope is approximately unchanged, as required by theory, except for conductivities as low as 10^{-12} mho/cm.

TABLE I. *Solutions of α-naphthylamine and phenol in xylene*

Logarithm of conductivity ratio	Emf, mv.
0.00	−30
0.78	0
1.39	0

TABLE II. *Solutions of picric acid in xylene plus 5 per cent ethyl alcohol*

Logarithm of conductivity ratio	Emf, mv.
0.62	410
1.07	450
1.34	370

In order to show that the silver myristate electrode reacts with aliphatic acids and not with a phenol in solution, a control test was carried out by using solutions of α-naphthylamine and phenol in xylene. Table I gives the result. It may be seen that the potentials do not follow any regular trend. A further proof for the specific action of the aliphatic acid electrode was furnished by using picric acid solutions in xylene plus 5 per cent ethyl alcohol. The emf data are presented in Table II. The high positive potentials show that the picric acid anions are inactive in contact with the myristate electrode.

For the measurements, the description of which follows, a hydrocarbon oil having a viscosity at 25°C. of 0.14 poise was used. In order to determine whether the electrode reaction is specific with regard to the chain length of the aliphatic acid, two acids, namely, propionic and myristic acids were investigated.

Concerning the *propionic acid* series, Table III gives the information on electric conductivity of the solutions. It was shown in a previous paper (1) that, in first approximation, an equation of the form

$$\sigma = k c_B^{n/2} c_A^{m/2} c_P^{l/2} \qquad (2)$$

may be used to reproduce the experimental data for a particular combination of compounds. Here c_B, c_A, and c_P are the molar concentrations of the amine, the acid, and the phenolic compound, k is a constant and n, m, and l are the number of molecules participating in the compound formation. An equation of this kind that fits the experimental data fairly well is given by:

$$\sigma = 20 \times 10^{-6} c_B^{1.5} c_A^{2} c_P^{2} \qquad (3)$$

from which it follows that 3 molecules of the amine, 4 of propionic acid, and 4 of *o*-cresol form an addition compound. Conductivities computed from Equation (3) are tabulated in the last column of Table III.

TABLE III. *Conductivity of propionic acid solutions in oil*

Concentration, millimoles/liter			Conductivity 10^{-12} mho/cm.	
Tributylamine	Propionic acid	o-Cresol	Measured	Calculated
20	80	200	5.6	14
32	80	200	14	29
50	80	200	47	57
80	80	200	145	120
80	20	200	4.5	7.2
80	32	200	14	18
80	50	200	53	45
80	80	200	140	120
80	80	40	4.1	4.6
80	80	70	11.5	14
80	80	120	44	42
80	80	200	145	120
30	30	200	4.7	3.7
40	40	200	12	10
60	60	200	47	42
80	80	200	115	120
4	80	100	8.6	10
52	80	130	21.5	26
64	80	160	49	53
80	80	200	115	120
80	40	100	7.1	7.2
80	52	130	21	21
80	64	160	52	47
80	80	200	130	120

The nature of the addition compound is uncertain; in all probability there is no water formed. The structure of the compound containing one molecule of each component may be visualized as follows:

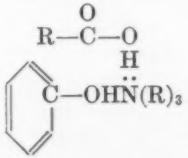

with the electron pair of the nitrogen resonating between the hydrogen atoms of the acid and the phenol.

The silver propionate for the silver electrode was prepared in a manner similar to that followed in preparing the myristate. Results of emf measurements are shown as Curve 1 of Fig. 3. The concentration of the phenol was the same on both sides of the cell. The curve has a reasonably constant slope, according to which t_c is about 0.64. This curve which forms the basis of subsequent measurements, will be called the standard propionate curve.

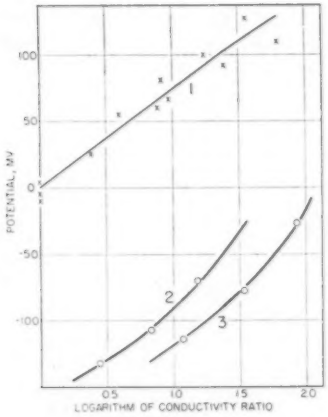

FIG. 3

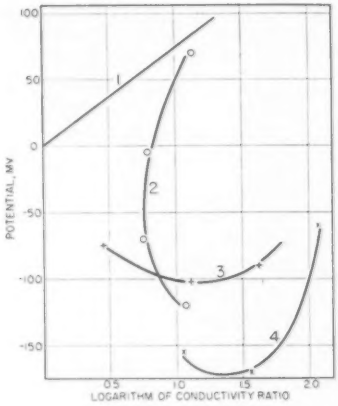

FIG. 4

FIG. 3. Emf vs. conductivity ratio for propionate solutions in oil. Curve 1, standard propionate curve; Curves 2 and 3, 0.12 m. phenolic differential.

FIG. 4. Emf vs. conductivity ratio for propionate solutions in oil. Curve 1, standard propionate curve; Curve 2, varying phenolic differential; Curves 3 and 4, varying degrees of dilution.

The two other curves, 2 and 3, Fig. 3, refer to data in which the variable solution contained less phenol than the reference solution. The curves are, therefore, shifted to negative values. The free energy of solvation of a mole of amine plus propionate ions is assumed to be proportional to the concentration of cresol and will be designated herein as Ac_P. Equation (1) then may be extended for a concentration differential of Δc_P in the following manner

$$E = 118\, t_c \log_{10} (\sigma_r/\sigma) - (At_c/F)\, \Delta c_P \qquad (4)$$

or, if A is measured in kg.-cal.,

$$E = 118\, t_c \log_{10} (\sigma_r/\sigma) - 43\, At_c\, \Delta c_P \qquad (5)$$

In order to justify the assumption that the effect is linear with Δc_P, a set of data was taken in which c_P was gradually decreased while the attempt was made to keep σ of the variable solution approximately constant. The

result of this series is shown in Curve 2 of Fig. 4. For each step Δc_P was 0.055 mole/liter. The shift of the potential is, indeed, linear in first approximation. The proportionality factor of Δc_P is 1500 mv. according to Fig. 3, and 1100 mv. according to Fig. 4. Taking the average, 1300 mv., and substituting in Equation (5):

$$1300 = 43\, t_c\, A,$$

one obtains for A, with $t_c = 0.64$, as found above, about 50 kg.-cal. per mole/liter cresol. Thus, in a solution of, say, 0.1 m. cresol the free energy of solvation of 1 mole of amine plus propionate ions is about 5 kg.-cal.

TABLE IV. *Composition and conductivity of diluted oils*

Composition or number of diluted oil	Dilution	Conductivity, 10^{-12} mho/cm.
0.08 m. tributylamine 0.08 m. propionic acid 0.12 m. o-cresol	1:1	52
Same	1:1.4	11.3
Same	1:2	3.5
0.08 m. tributylamine 0.08 m. propionic acid 0.08 m. o-cresol	1:1	19
Same	1:1.4	5.9
Same	1:2	1.8
Oil No. 2	1:1	19
Oil No. 2	1:2	6.2
Oil No. 2	1:4	1.9
Oil No. 3	1:1	27
Oil No. 3	1:1.4	7.8
Oil No. 3	1:2	2.6

With the information obtained so far, the trend of the potential obtainable from a series of increasing dilutions with pure oil of a particular solution may be predicted. According to the first term of Equation (5) E will increase; according to the second term E will decrease. Hence, a relatively small change of E may be expected. Curve (3) of Fig. 4 shows this to be the case. The composition and conductivity of the two series are tabulated in the first two groups of Table IV; we shall return to the two last groups later. Actually, all dilution curves show a concavity upward, while in the range of lower conductivities ($\sim 10^{-12}$) the rise becomes rather sharp. The trend of the dilution curve could be computed using Equation (5), but the accuracy of the measurements is not sufficiently high to warrant such computations.

A solvent effect on the potential has been mentioned herein only in relation to the phenolic compound. Actually, the other two components also have specific effects which appear to be roughly of equal magnitude and opposite sign, as will be shown. Thus, if both amine and acid are equimolar, the only solvent effect left is that due to the phenolic compound. If, however, the amine and acid are not present in equimolar concentra-

tions, additional solvent effects are exhibited. These conditions are shown in Fig. 5. The six curves drawn through the measured points refer to the six sets of solutions, the composition and conductivity of which were tabulated in Table III. Curve 2 refers to equimolar amounts of the amine and acid and a decreasing amount of *o*-cresol; the cresol effect is clearly shown. Curve 3 refers to solutions in which only the propionic acid content was gradually decreased. There is a depression with regard to the standard curve, the proportionality constant being about 1300, the same as for cresol. Curve 4 refers to solutions in which only the amine content was reduced; one observes a positive term of a somewhat lower absolute magnitude than the term for Curve 3 in which the acid is the variable.

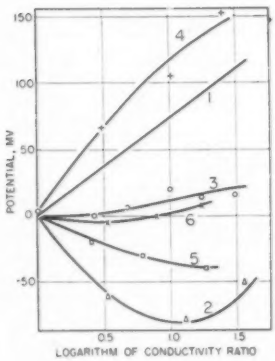

FIG. 5

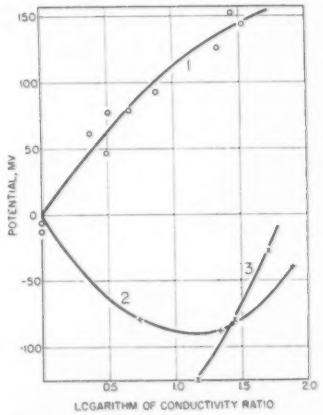

FIG. 6

FIG. 5. Solvent effect on potential for propionate solutions in oil. Curve 1, standard propionate curve; Curve 2, varying concentration of o-cresol; Curve 3, varying concentration of propionic acid; Curve 4, varying concentration of amine; Curve 5, varying concentration of acid and cresol; Curve 6, varying concentration of amine and cresol.

FIG. 6. Emf data for myristate solutions in oil. Curve 1, standard myristate curve; Curve 2, varying concentration of *o*-cresol; Curve 3, $\Delta c_p = 0.15$.

Curves 5 and 6 show combination effects. In the series reproduced by Curve 5, both the acid and cresol content were decreased; the curve lies between Curves 2 and 3. In reference to Curve 6, both the amine and cresol content were decreased, and the curve lies between Curves 2 and 4.

With regard to the *myristic acid* series in the same oil, Table V gives data on the electrical conductivity. Equation (2) takes the following form for this case:

$$\sigma = 1.4 \times 10^{-6}\, c_B^{1.5}\, c_A\, c_P^{2.5} \qquad (6)$$

The numbers of molecules forming the compound are respectively: 3, 2, and 5. The constant is smaller than in Equation (3), indicating lower conductivities for identical concentrations. Emf data for the myristic acid series are reproduced in Fig. 6. Curve 1 gives the standard myristate

curve referring to equimolar amounts of the acid and base. From the average slope, t_c about 0.85 follows, a value higher than for the propionate series. On the basis of the greater length of the myristate chain, this difference is explainable. Curve 2 refers to a series in which only the *o*-cresol content was reduced; it shows the solvent effect of cresol. When c_P is constant and lower than in the reference solution, the curve obtained has a slope similar to that of Curve 1, only shifted to lower potentials. Curve 3 refers to $\Delta c_P = 0.15$.

TABLE V. *Conductivity of myristic acid solutions in oil*

Concentration, millimoles/liter			Conductivity, 10^{-12} mho/cm.	
Tributylamine	Myristic acid	*o*-Cresol	Measured	Calculated
120	120	40	2.2	2.3
120	120	70	7.6	9.2
120	120	120	31	35
120	120	220	170	160
53	53	100	4.4	2.9
80	80	100	8.3	8.0
120	120	100	16	22
53	53	250	25	28
80	80	250	82	76
120	120	250	190	220

TABLE VI. *Comparison between propionate and myristate electrodes in the same solution*

Type of variable solution	Type of electrode in variable solution	Log of σ ratio	Emf, in mv.
Propionate	Ag propionate	0.0	−10
Propionate	Ag propionate	0.60	+55
Propionate	Ag propionate	1.24	+100
Propionate	Ag myristate	0.0	+12
Propionate	Ag myristate	0.56	+60
Propionate	Ag myristate	1.16	+98
Myristate	Ag propionate	0.0	+2
Myristate	Ag propionate	0.37	+60
Myristate	Ag propionate	0.88	+126
Myristate	Ag myristate	0.0	−6
Myristate	Ag myristate	0.37	+61
Myristate	Ag myristate	0.88	+122

The use of two different aliphatic acids in the various solutions enabled the determination of the degree of specificity with regard to chain length of the electrode reaction. Table VI shows some of the results. As may be seen, the potentials are essentially the same. The chain length appears to have little effect, if any, upon the reaction, presumably because by exchange a small amount of silver propionate is formed in the presence of propionic acid and silver myristate—and vice versa.

The following test shows that the aliphatic electrode does not react with

another type of acid in hydrocarbon oil, namely sulfonic acids. Solutions of lauryl sulfonic acid in oil containing 0.25 m. *o*-cresol were used. The result is shown in Table VII.

The high positive potentials indicate that the aliphatic anion concentrations were exceedingly low; the sulfonic acid anions, present in large concentrations, were inactive in contact with the myristate electrode.

The essential role of the silver salt was demonstrated in the following experiment. Propionate solutions were used and the variable solution was in contact with a bright silver electrode. The emf data, shown in Table VIII, are considerably below the standard curve level.

Having shown that the negative ions in the above discussed solutions are phenol-solvatized anions of aliphatic acids, the attempt was made to check, in this regard, oils that have been oxidized. The results are shown in Fig. 7. An interpretation of these data is difficult inasmuch as in an oxidized oil not only the nature of the electrolytes, but also that of the solvents, is unknown. Curves 1 and 2 are the standard propionate and

TABLE VII. *Solutions of lauryl sulfonic acid in hydrocarbon oil*

Logarithm of conductivity ratio	Emf, mv.
0.11	350
0.55	300
0.94	260

TABLE VIII. *Emf data with bright silver electrode in variable propionate solution*

Logarithm of conductivity ratio	Emf, mv.
0.0	−310
0.56	−270
1.16	−250

myristate curves, reproduced for the sake of comparison. The dotted curves, 3 and 4, present data for three different oxidized oils (No. 1, 2, 3), with conductivities respectively: 2.5×10^{-12}, 1.5×10^{-11}, and 3.0×10^{-11} mho/cm. For Curve 3 the propionate and for 4 the myristate reference electrodes were used. Absence of the electrode ions would result in a potential higher than the standard curve level; the location of the measured points below the standard curves indicates the possible presence of the electrode ions. The fact that the points do not lie on the standard curve is explainable on the basis of the solvent effect. The depression appears to be due to a differential in the concentration of the solvatizing compound. It appears that this latter, at least in the oils examined, was not a phenolic compound since the phenol reaction with 2-6 dibromoquinone chloro-imide was negative. Considering the two oils of highest conductivity, the depression of the propionate data is about 180 mv., corresponding to $\Delta c_P = 0.14$. Since the reference solution contained 220 millimoles of cresol, the solvating level of the two oxidized oils corresponds to about 80 millimoles per liter.

Next, dilution data of the two oils of highest conductivity were taken.

The conductivities at given dilutions with pure oil are shown in the two last groups of Table IV. It may be noted that the σ data of Oil No. 3 are similar to those of the triple solutions, whereas the degree of dilution necessary to produce the same values of σ is pronouncedly larger for Oil No. 2. This indicates that the ion-forming compounds are rather different in Oils 2 and 3. The emf data for these dilutions are shown in Curves 5 and 6, Fig. 7. They are rather similar to the dilution curves, 3 and 4, Fig. 4. If measured potential differences are due to the aliphatic anions in the oxidized oil, an addition of cresol should raise the potential. Results with Oil No. 2 are shown in Curve 2, Fig. 8. Each step corresponds to 0.05 m.

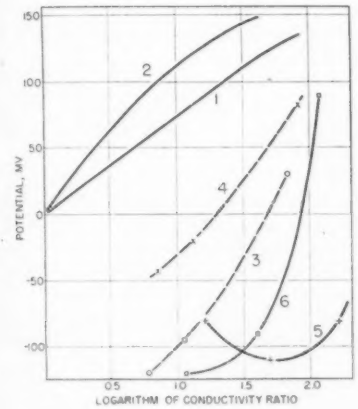

FIG. 7

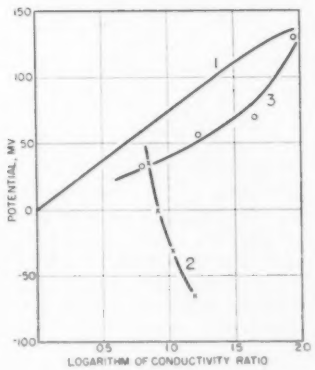

FIG. 8

FIG. 7. Emf vs. conductivity ratio for oxidized hydrocarbon oils. Curve 1, standard propionate curve; Curve 2, standard myristate curve; Curve 3, Oils 1, 2, 3 vs. propionate reference electrode; Curve 4, Oils 1, 2, 3 vs. myristate reference electrode; Curve 5, Dilution, Oil 2 vs. propionate reference electrode; Curve 6, Dilution, Oil 3 vs. propionate reference electrode.

FIG. 8. Emf vs. conductivity ratio for oxidized hydrocarbon Oil No. 2. Curve 1, standard propionate curve; Curve 2, varying phenolic addition to Oil 2; Curve 3, Oil 2 diluted; *o*-cresol content 0.20 m.

o-cresol; the potential at 0.15 m. *o*-cresol approaches the level of the standard propionate curve (Curve 1). Since the *o*-cresol content of the reference solution was 0.25 m., the solvating level of the oxidized oil is about 0.10 m., as concluded earlier. If, then, the level of Oil 2 is raised sufficiently to bring it to standard level, dilution with pure oil containing the same phenolic level should result in a curve not too different from the standard propionate curve. This measurement was carried out with an added *o*-cresol content of 0.20 m. The result is given by Curve 3, Fig. 8, which reasonably substantiates our conclusion.

These tests may be taken as an indication that the negative ions in oxidized oils are solvated anions of aliphatic acids. It is possible that the statement holds true for only part of the existing ions in oxidized oils.

The present study was concerned with the electrochemical identification

of negative ions in hydrocarbons. It might be of interest to find a reversible electrode for the positive ions; it would form the counterpart to the aliphatic electrode described.

Any discussion of this paper will appear in the discussion section of Volume 94 of the Transactions of the Society.

REFERENCES

1. Andrew Gemant, *J. Chem. Phys.*, **14**, 424 (1946).
2. Samuel Glasstone, *Textbook of Phys. Chemistry*, p. 923, D. Van Nostrand Co., New York, (1947).
3. Andrew Gemant, *J. Chem. Phys.*, **13**, 146 (1945).

REACTIONS OF MOLTEN TITANIUM WITH CERTAIN REFRACTORY OXIDES.[1]

PORTER H. BRACE

Westinghouse Research Laboratories, East Pittsburgh, Pennsylvania

ABSTRACT

Titanium metal was melted in vacuo in contact with Al_2O_3, BeO, and ThO_2 respectively. The metal reacted vigorously with Al_2O_3, less so with BeO, and slightly with ThO_2. Qualitatively, the relative positions of the oxides on the scale of reactivity with titanium are consistent with the oxygen dissociation pressures as calculated from thermochemical data.

It was concluded that of the three oxides studied only thorium oxide showed any promise as a crucible material for melting titanium or titanium-base alloys.

INTRODUCTION

The problem of refractories to contain titanium is one of some difficulty and the experimental work here reported was undertaken with the object of learning the relative merits of oxides of aluminum, beryllium, and thorium as materials for crucibles in which to melt titanium and titanium-base alloys.

Both the heat of oxidation and the melting temperature of titanium are relatively high and in the molten state it reacts vigorously with most oxides. Titanium also has the property of dissolving a certain amount of oxygen, a circumstance that may contribute significantly to its activity with respect to the oxides of other metals.

EXPERIMENTAL

The construction of the vacuum "furnace" employed in this study is indicated in Fig. 1. A fused-silica tube, *A*, approximately 5 in. (12.7 cm.) I.D. by 36 in. (91 cm.) long with smoothly ground end-surfaces was held between water-cooled brass end-pieces, *B*, *C*, which were grooved to hold "Neoprene" gaskets, *D*, the latter forming effective vacuum sales under compression exerted by tie-rods, *E*, attached to the end-pieces.

[1] Manuscript received April 17, 1948. This paper presented at the Columbus, Ohio Meeting, April 14 to 17, 1948.

The heating element comprised a capsule, *F*, and sight-tube, *G*, machined from sintered molybdenum compacts supplied by Westinghouse Lamp Division. Granules of electrically-fused thorium oxide (10–20 mesh) filled the annular space between the quartz vacuum tube and the heating element, supporting the latter and also providing fairly effective thermal insulation.

Exhaust was effected by means of a 4 in. (10.2 cm.) Westinghouse oil-vapor pump and booster supported by a Cenco "Hypervac 20" mechanical pump. Pressures down to 1×10^{-5} mm. Hg (.01 micron) as measured by McLeod gauge were attainable at the upper end of the quartz tube (i.e., as

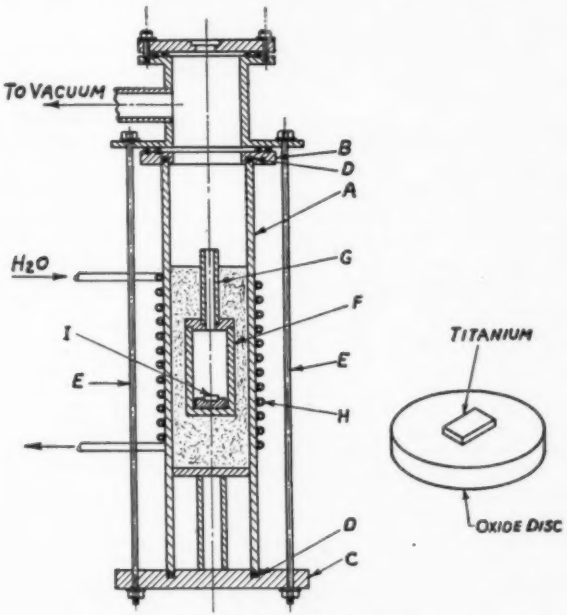

FIG. 1. Experimental furnace

close as possible to the scene of action) when the system was cold. On heating, however, disengagement of gas from the refractories, metal, and the internal surfaces of the furnace was so rapid that pressures approximating 1×10^{-1} mm. Hg (100 microns) developed unless the temperature was increased gradually.

The molybdenum capsule was heated by induction from an axially-movable coil, *H*, that surrounded the furnace tube and was energized at 9.6 kc. by a Westinghouse motor-alternator set. It was found that very satisfactory temperature control was obtainable by manual adjustment of the excitation of the alternator. Temperature distribution along the capsule could be altered by moving the coil axially as required. Estimates

of the temperature of the test-specimen, I, were made by means of a Leeds & Northrup optical pyrometer sighted through a Pyrex glass observation window in the top cover-plate of the furnace.

Materials

1. *Aluminum oxide.* A white, micro-crystalline powder of high-purity Al_2O_3 obtained from Aluminum Company of America. This is a grade often used for refractory insulation and appeared to be substantially free of alkalis, silica, and heavy metal oxides.

2. *Beryllium oxide.* A very fine white powder of the exceptionally pure oxide used in fluorescent lamps. It was obtained through the Research Department of Westinghouse Lamp Division.

3. *Thorium oxide.* A specially purified product from Maywood Chemical Company in the form of fine white powder that yielded a small amount of water when calcined.

Although none of the oxides used were subjected to quantitative chemical analysis at our Laboratories, we are confident that no significant amounts of extraneous material were present.

4. *Titanium.* The titanium was obtained from Titanium Alloys Manufacturing Company. As received it was in the form of discs of fused metal approximately 8 in. (20.3 cm.) in diameter and $\frac{1}{2}$ in. (1.27 cm.) thick. These were the product of the reduction of titanium tetrachloride by alkali-metal in a closed reaction-chamber, fusion having been effected by the surplus heat of reaction.

Our analysis of the metal gave the following results:

Element	Weight per cent
Si	1.09
V	0.29
Pb	0.15
Fe	0.61
Al	0.05
Cu	0.50
Mn	0.01
Total	2.70
Ti	Balance

Procedure

The finely divided oxides, slightly moistened, were compacted between flat-ended plungers in a steel die under pressures approximating 20,000 PSI (1,400 kg./cm.^{2}) to form discs 1 in. (2.54 cm.) in diameter and $\frac{3}{8}$ in. (0.95 cm.) thick. These were prepared for test by sintering in vacuum at temperatures in the neighborhood of 1700°C. in a molybdenum capsule and arranged as described previously. Heating periods of approximately 2 hours sufficed to develop considerable strength and a texture such that the compacts could be tooled to desired shapes.

A rectangular cavity approximately $\frac{1}{8}$ in. (.32 cm.) deep and $\frac{5}{16}$ in. (.79 cm.) wide and $\frac{5}{8}$ in. (1.59 cm.) long was formed in one face of each disc. This served to locate and confine the test-specimen before and after melting. The titanium specimens, machined from the discs as received, were parallelepipeds approximately $\frac{3}{16}$ in. (0.48 cm.) thick and of such lateral dimensions as to fit with a small clearance into the cavities in the discs.

The experiments were carried out by placing the disc bearing its little

block of titanium on the bottom of a molybdenum capsule. The capsule and sight tube were then assembled and mounted with the granular thoria thermal insulation within the furnace tube. It was found advantageous to outgas the thoria granules just prior to use by heating in air at approximately 1000°C. The furnace then was exhausted, cold, to a pressure of a few microns and the capsule heated to successively higher temperatures while pumping was continued, the heating rate being so adjusted as to keep pressures below approximately 5 microns as measured by a thermocouple-type vacuum gauge. The specimen was kept under observation through the telescope of the optical pyrometer until it appeared that melting had occurred. The high-frequency power then was shut off and the test material allowed to cool with the furnace, the pumps being kept in operation. Final pressures were quite low—of the order of 0.01 micron—and the test pieces usually came from the furnace with superficial discoloration as the only evidence of attack by the furnace atmosphere.

TABLE I. *Relative malleability of specimens of fused titanium*

Mark	Specimen	Remarks
A	Original	Strong and malleable
B	Suspended globule	Strong and malleable but perhaps slightly less ductile than A
C	Melted in contact with Al_2O_3	Extremely brittle, weak and friable
D	Melted in contact with BeO	Quite brittle, but showed some strength
E	Melted in contact with ThO_2	Noticeably harder and but slightly less malleable than A but, nevertheless, comparable as to mechanical properties

A separate test, however, was made to learn whether or not the reaction between the residual gases and the titanium was extensive enough to affect markedly the properties of the latter. A rectangular bar approximately $\frac{3}{8}$ in. (.95 cm.) square by 3 in. (7.6 cm.) long was machined from the original titanium disc and was suspended by a molybdenum wire from a cross-bar in the upper part of the furnace so that it hung coaxially in the molybdenum capsule with its long axis vertical, and the lower end a short distance above the bottom of the capsule. Then the capsule was heated under vacuum, until superficial fusion of the lower portions of the test-piece occurred and the molten metal drained downward to form a globule held by surface tension to the end of the specimen. Thus a small quantity of metal was obtained that had been melted while in contact only with itself and the furnace atmosphere.

Results

The results of this frankly qualitative study may be summarized as follows: (1) The contamination of the molten titanium by residual furnace gases was relatively unimportant; (2) The reaction of molten titanium with Al_2O_3 was vigorous, with BeO quite noticeable and with ThO_2 slight but, as indicated by wetting of the oxide by the metal, perceptible.

Tests of the specimens of fused metal were made with a hammer in order to compare their mechanical properties. The results are given in Table I.

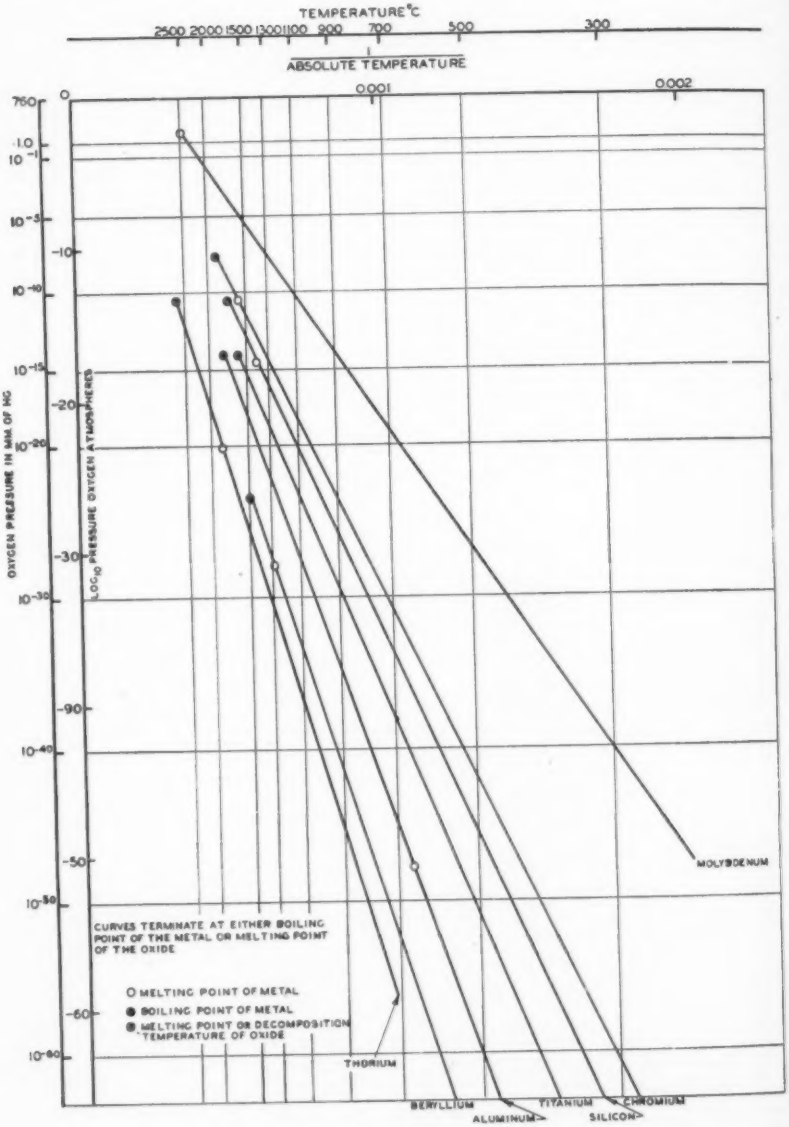

FIG. 2. Dissociation pressures of metal oxides

DISCUSSION

A reproduction of a chart prepared in collaboration with Dr. B. Lustman of the Westinghouse Research Laboratories (Fig. 2) shows the oxygen dissociation pressures of a number of oxides at various temperatures. The chart shows that titanium oxide has a higher dissociation pressure than any of the group, Al_2O_3, BeO, and ThO_2. On that basis alone it was not to be expected that titanium metal would show marked reducing action with respect to any one of those oxides unless the respective metals were being removed from the scene of action by vaporization or otherwise. Although vaporization cannot be ruled out, it is believed that it played no important part even in the most spectacular case, namely that of Al_2O_3, inasmuch as the action was so rapid that a visible rise of temperature occurred as soon as the titanium melted, and the titanium became so highly alloyed that the product bore no resemblance to either of the metals concerned. Perhaps Al-Ti intermetallic compounds were formed with sufficient energy of reaction to remove effectively from circulation the reduced aluminum and thus give rise to a trend opposite that to be expected from the oxygen dissociation data.

TABLE II. *Equilibrium concentrations in titanium at 1900°C. of metals from oxides noted*

Oxide	Equilibrium concentration in titanium (Mole fraction)
Al_2O_3	0.16
BeO	1.73×10^{-4}
ThO_2	74×10^{-9}

The embrittlement of the specimen melted in contact with BeO suggests that some transfer of Be occurred and that intermetallic compound formation may have played a part in this case also.

With thorium oxide the situation appears to be more nearly in line with what would be expected from the oxygen dissociation pressure data, although even here more Th appears to have passed into the Ti than might have been anticipated.

The equilibrium concentrations of the Al, Be, and Th respectively in liquid Ti at 1900°C. (melting point of Ti assumed to be 1800°C.) in contact with the oxides of the first-named metals are shown in Table II.[2]

CONCLUSIONS

1. Reduction of the oxides, Al_2O_3, BeO, and ThO_2 by molten titanium in vacuum proceeds far beyond the limits that might be expected from the oxygen dissociation pressures as calculated for the oxides at the melting point of titanium.
2. Al_2O_3 and BeO would be useless as crucibles for melting titanium.
3. Thorium oxide appears to offer some promise as a crucible material although it cannot be regarded as inert to molten titanium.
4. It is proposed that the formation of intermetallic compounds between

[2] Based on private communication from Dr. A. E. Gulbransen, Westinghouse Research Laboratories. These figures should be regarded as estimates only.

titanium and the metals liberated from the oxides in question accounts for the unexpectedly great reducing power shown by molten titanium.

ACKNOWLEDGMENTS

The writer wishes to thank the several members of the staff of Westinghouse Research Laboratories who have aided in the preparation of this paper and to acknowledge in particular his indebtedness to Mr. Don R. Mosher for assistance in carrying out the experimental work, and to Dr. B. Lustman and Dr. E. A. Gulbransen for helpful comments and data concerning the thermodynamic questions involved.

Any discussion of this paper will appear in the discussion section of Volume 93 of the Transactions of the Society.

ELECTRODEPOSITION OF NICKEL FROM ORTHOPHOSPHATE BATHS[1]

C. B. F. YOUNG

Brooklyn Polytechnic Institute, Brooklyn, New York

AND

E. S. ROSZKOWSKI

58-59 43rd Ave., Woodside, New York

ABSTRACT

Mat and adherent nickel deposits which could be buffed to a bright finish have been successfully electrodeposited from a solution containing nickel phosphate and phosphoric acid in various amounts at temperatures ranging from 25°C. (75°F.) up to 85°C. (185°F.) and at current densities varying from 20 to 1200 amp./sq. ft. (2.2 to 130 amp./sq. dm.). In general, the current efficiencies were lower than those given by sulfate-chloride baths. Addition and wetting agents as a rule were found to be detrimental to the deposits. The electrolyte was prepared by dissolving at 105°C. (221°F.) a C. P. grade of nickelic oxide, possessing an amorphous microstructure, in a solution of phosphoric acid, sp. gr. 1.379, and diluting the result to the desired concentrations after the proper additions of alkali phosphate which served to increase the conductivity, increase the plating efficiency, and decrease the plating range.

HISTORIAL REVIEW

The purpose of this investigation was to explore the possibilities of using a complex phosphate bath to deposit nickel. Phosphate baths, with few exceptions, have found very limited use commercially with the exception of those for the platinum metals. On the other hand, the literature con-

[1] Manuscript received February 19, 1948. This paper, which is part of a thesis submitted by E. S. Roszkowski in partial fulfillment of the requirements for the degree of Doctor of Chemical Engineering at the Brooklyn Polytechnic Institute, prepared for delivery before the New York Meeting, October 13 to 16, 1948.

tains many references on the use of phosphates in baths. This review considered only articles which dealt with phosphate baths *per se*. References where phosphates were used simply as addition salts have been ignored.

Maigne and Mathey (1) proposed a bath which contained essentially nickel salts other than phosphates and monobasic ammonium phosphate. Koyonagi (2) proposed the use of a number of electrolytes which contained essentially the salt of the metal to be plated and an alkali pyrophosphate.

Langbein (3) suggested the use of an electrolyte containing:

	g./l.	oz./gal.
Nickel phosphate, $Ni_3(PO_4)_2 \cdot 7H_2O$	19.0	2.53
Nickel pyrophosphate, $Ni_2P_2O_7 \cdot 6H_2O$	80.0	10.67

For deposition on copper cathodes, a current density of 0.5 amp./sq. dm. (4.65 amp./sq. ft.) at 3.5 volts was used. For deposition on zinc, a current density of 0.55 amps./sq. dm. (5.11 amp./sq. ft.) at 2.8 volts was used. The voltages specified were on electrodes spaced 10 cm. apart.

Powell (4) suggested an electrolyte containing:

	g./l.	oz./gal.
Nickel phosphate, $Ni_3(PO_4)_2 \cdot 7H_2O$	22.5	3.0
Sodium pyrophosphate, $Na_2P_2O_7$	26.2	3.5
Nickel citrate, $Ni_3(C_6H_5O_7)_2$	15.0	2.0
Ammonium hydroxide, NH_4OH (sp. gr. 0.9362)	37.5	5.0

In a subsequent patent, Powell (5) used an electrolyte containing:

	g./l.	oz./gal.
Nickel phosphate, $Ni_3(PO_4)_2 \cdot 7H_2O$	15.0	2.0
Nickel citrate, $Ni_3(C_6H_5O_7)_2$	15.0	2.0
Nickel sulphate, $NiSO_4 \cdot 6H_2O$	34.0	4.53
Benzoic acid, C_6H_5COOH	7.5	1.0

It was claimed that the benzoic acid acted as a stabilizer.

The only other mention of nickel phosphate was that of Maigne and Mathey (1). The compositions of two electrolytes were given without specification as to dilution. This was assumed to be one liter as shown below. The second solution was attributed to Powell (5). The compositions were as follows:

Solution 1

	g./l.	oz./gal.
Nickel phosphate, $Ni_3(PO_4)_2 \cdot 7H_2O$	14.0	1.87
Nickel citrate, $Ni_3(C_6H_5O_7)_2$	14.0	1.87
Nickel acetate, $Ni(C_2H_3O_2)_2 \cdot 4H_2O$	14.0	1.87
Nickel chloride, $NiCl_2 \cdot 6H_2O$	14.0	1.87
Benzoic acid, C_6H_5COOH	7.0	0.93

Solution 2

Nickel phosphate, $Ni_3(PO_4)_2 \cdot 7H_2O$	7.0	0.93
Nickel citrate, $Ni_3(C_6H_5O_7)_2$	20.0	2.67
Nickel acetate, $Ni(C_2H_3O_2)_2 \cdot 4H_2O$	20.0	2.67
Sodium bisulphite, $NaHSO_3$	7.0	0.93
Ammonium hydroxide, NH_4OH (sp. gr. 0.9362)	32.5	4.34
Trisodium phosphate, $Na_3PO_4 \cdot 12H_2O$	14.0	1.87

In addition to the orthophosphate, the pyrophosphate bath has been suggested. Langbein suggested one solution of the composition given above and, in a later publication (6), suggested a solution containing:

	g./l.	oz./gal.
Nickel pyrophosphate, $Ni_2P_2O_7 \cdot 6H_2O$	19.48	2.5
Sodium pyrophosphate, $Na_4P_2O_7 \cdot 10H_2O$	79.4	10.6

This solution was operated at 0.5 amp./sq. dm. (4.65 amp./sq. ft.) at 3.5 volts with electrodes spaced 10 cm. apart.

Levy (7) discussed an alkaline bath (soda, potash, etc.) with slight additions of alkaline cyanides in conjunction with an anode of the metal. In place of the cyanide, phosphates and pyrophosphates were also used with or without the addition of sodium bisulphite or sodium sulphite.

A close study of the literature did not show the existence of a commercial phosphate bath for the deposition of nickel. The present work was based on the fact that nickel phosphate is soluble in solutions of acids and ammonium salts.

PREPARATION OF THE ELECTROLYTE

A mixture, containing 650 cc. (0.1717 gal.) of phosphoric acid (sp. gr. 1.689) and 650 cc. (0.1717 gal.) of water, was heated to a temperature of 100–110°C. (212–230°F.). The boiling point of the solution was 110°C. (230°F.). At lower temperatures, the rate of dissolution was very slow. To the solution of acid at the elevated temperature was added, in stages, 195 g. (6.88 oz.) of nickelic oxide. Small additions were necessary because of considerable effervescence caused by the evolution of large amounts of oxygen formed in the transformation of trivalent nickel oxide to bivalent nickel phosphate. A test for oxygen was obtained. The reaction

$$6Ni_2O_3 + 8H_3PO_4 = 4Ni_3(PO_4)_2 + 12H_2O + 3O_2$$

required a minute or two to start, and once started, progressed exothermically maintaining the required temperature. If the oxide was added too rapidly, the combined effects of the gas evolution and boiling caused the reacting mixture to overflow. After the dissolution had been completed, the solution was diluted to 2400 cc. (0.634 gal.) and filtered while hot through asbestos fiber pad on a Buchner funnel. After filtering, the solution was diluted to the final volume of 2600 cc. (0.637 gal.) and had a composition of:

Nickelic oxide, Ni_2O_3	75 g./l.	10 oz./gal.
Phosphoric acid, H_3PO_4 (sp. gr. 1.689)	250 cc./l.	1 qt./gal.

Weight of the nickelic oxide as starting material was specified for this and subsequent compositions instead of the exact quantity of the reaction product. The stock solution of this composition was diluted until the desired compositions were obtained.

The above procedure resulted from a study of the variables encountered in the process. The effect of acid dilution in the preparatory stage was also considered. The use of phosphoric acid, sp. gr. 1.689 or sp. gr. 1.475, resulted in a solid mass of the hydrated phosphate products. These

materials were very difficult to dissolve. At the dilution specified, the reacting mixture was always a liquid at the given temperature. At dilutions much below the specified values, the rate of solution was almost nil. The final concentration of the stock solution was selected so that salts would not crystallize when the solution cooled to room temperature. The amount of nickelic oxide added per unit of phosphoric acid was determined so that the content of nickel in solution was as high as possible producing a complete solubility of the oxide. Additions of the oxide in excess of the specified value resulted in a partial solubility.

One other limiting factor was noted. A chemically pure nickelic oxide from one source[2] had a very fine, amorphous structure when observed under a microscope (128 ×). A technical grade of nickelic oxide as supplied by another source[3] proved to be insoluble. The structure of the latter material at a magnification of 128× proved to be coarse, granular and, at times, transparent appearing as if it had been fused. A chemically pure grade of nickelous oxide obtained from the first source[2] also proved to be insoluble, and its microstructure was found to be of a granular type. A number of samples of nickelic oxide with the amorphous microscopic structure were tried and all proved to be soluble. This led to the conclusion that the oxide with the amorphous structure was the only one useable. This view was further supported by the generally prevalent opinions that oxides lose their solubility on fusion. No troubles were encountered with the use of a commercially supplied phosphoric acid (sp. gr. 1.579).[3]

The preparation of the electrolyte was not limited to the one method given above. An electrolyte was also prepared by dissolving a pure grade of nickelous phosphate in phosphoric acid, due allowance having been made in regard to the stoichiometric relationships, so that the same stock solution was obtained. The nickelous phosphate could also be prepared by precipitation with trisodium phosphate from a nickel salt solution. Since the nickelous phosphate was insoluble in the precipitating solution, it could be completely removed.

The stock solution was mixed with various alkali phosphates and diluted in accordance with requirements. For example, to 100 cc. of the stock nickel solution, 20 grams of trisodium phosphate were added and the result was diluted to 200 cc., producing a solution having the following composition:

Nickelic oxide, Ni_2O_3	37.5	g./l.	5 oz./gal.
Phosphoric acid, H_3PO_4(sp. gr. 1.689)	125	cc./l.	1 pt./gal.
Trisodium phosphate, $Na_3PO_4 \cdot 12H_2O$	100	g./l.	13.33 oz./gal.

This solution had a pH of 2.2, as measured by a glass electrode and contained 0.45 mole of nickel, 1.83 moles of phosphoric acid, and 0.263 mole of trisodium phosphate per liter. Attempts to vary the pH by further addition of phosphoric acid increased the total acid content without an appreciable change in the pH.

The pH could be raised by the addition of ammonium hydroxide or sodium hydroxide, but if the value was much above 2.2, a precipitate of nickel phosphate formed. Further, when sufficient ammonia was added,

[2] Purchased at Eimer and Amend, New York City.
[3] Purchased at City Chemical Company, New York City.

the deep blue amino complex resulted. The amount of base added was found to be a function of the concentration of the trisodium phosphate in solution. The decrease in the amount of a base tolerated by a given solution was directly proportional on an equivalent weight basis to the increase in the amount of trisodium phosphate in solution.

Another point which should be mentioned is the relationship between the amount of trisodium phosphate present in the solution and the total acid content of the bath. The trisodium phosphate tolerance was increased by increasing the amount of phosphoric acid in amount sufficient to form the monobasic salt from the tribasic compound, leaving an excess of acid which served to increase the free acid content of the solution. On the basis of using 100 cc. of stock nickel solution in a 200 cc. bath, the salt tolerance was as indicated below:

Additional H_3PO_4 (sp.gr. 1.689) *cc.*	$Na_3PO_4 \cdot 12H_2O$ tolerated *g.*	Calculated free acid content *cc.*
0	20	5.47
10	32	8.15
16.67	40	20.56

The free acid content necessary to maintain the salts in solution is also indicated above.

The final relationship considered was the effect of the dilution of the stock nickel solution on the tolerance of trisodium phosphate. On a basis of a final volume of 200 cc., the tolerance was found to be as follows:

Stock nickel solution used *cc.*	Salt added *g.*	Free acid content in cc. of sp. gr. 1.689
200	40	11.48
150	30	8.61
100	20	5.47
50	10	2.87
25	0	3.15

Computation of the free acid in the same manner as before showed a free acid content as shown above. This further gave the relationship between the salt tolerance and the free acid content of the bath.

EXPERIMENTAL

Cell

The cell consisted of a 250-cc. beaker containing 200 cc. of an electrolyte. Each solution was discarded after a set of runs was made. Corrections for evaporation were made when required to maintain the volume within three per cent. The temperature of the cell was maintained within ± 1.5°C. (2.7°F.) of the operating temperature.

The anode was a thin nickel sheet, 0.75 inch (1.90 cm.) wide by 3 inches (7.62 cm.) long, having a submerged area (2 in. by 0.75 in., 5.08 cm. by 1.90 cm.) of 1.5 sq. in. (9.68 sq. cm.) since, in resting against the side of the beaker, the back of the anode was shaded.

The cathode was an 18-gauge (0.040 in., 1.016 cm.) polished copper strip, two inches (5.08 cm.) long by 0.75 inch (1.90 cm.) wide and had an effective submerged area of 1.5 sq. in. (9.68 sq. cm.). The cathode was supported in

the electrolyte by a wire. To permit higher current densities than possible with the above-sized cathode, a copper strip was used which was 0.75 inch by 1.25 inches (1.90 cm. by 3.18 cm.) and which had an effective submerged area of 0.9373 sq. in. (6.04 sq. cm.).

Plating cycle

The following plating cycle was set up:

1. Clean in electro-cleaner
2. Rinse in cold water
3. Acid dip
4. Rinse in cold water
5. Clean in electro-cleaner
6. Rinse in cold water
7. Dry
8. Weigh
9. Clean in electro-cleaner
10. Rinse in cold water
11. Nickel plate
12. Rinse in cold water
13. Dry
14. Weigh

A constant number of coulombs was used, and deposition for 5 ampere minutes was found sufficient to give enough plate to be used in calculating the efficiencies.

Electrolyte control

With the use of the soluble anode, bath compositions at the higher concentrations did not vary more than two per cent. This permitted a number of runs to be made with each sample of solution.

PRELIMINARY WORK

In the preliminary work, the bath contained 100 cc. of stock nickel solution in 200 cc. of the bath. Deposits were obtained at 60°C. (140°F.) when current densities in the vicinity of 300 amp./sq. ft. (32.4 amp./sq. dm.) were used.

In studying the effect temperature, the results of three runs using 340 amp./sq. ft. (35.7 amp./sq. dm.) showed that the higher temperatures favored higher current efficiencies. The above bath gave an efficiency of 15 per cent at 25°C. (77°F.) and an efficiency of 50 per cent at 85°C. (185° F.). Further preliminary work was then done at 85°C. (185°F.).

At 340 amp./sq. ft. (35.7 amp./sq. dm.). increase in phosphoric acid concentration reduced the current efficiency of plating. The original bath gave an efficiency of 52.2 per cent, whereas an addition of 10 cc. of the acid decreased the efficiency to 28.2 per cent, and a further addition of 10 cc. decreased the efficiency to 7.23 per cent.

Going to the other extreme, ammonium hydroxide was added, and at first, the efficiency increased with the slight additions, but with subsequent increases, the efficiency decreased. Further additions of ammonium hydroxide caused a formation of a precipitate which redissolved when a sufficient amount of ammonium hydroxide had been added to form the deep blue amino complex. After the addition of 10 cc. of 6 normal ammonium hydroxide the efficiency was 58.4 per cent. A further addition of 2½ cc. increased the efficiency to 87 per cent whereas a second addition of 2½ cc. decreased the efficiency to 54.7 per cent. Further addition of ammonia caused a precipitate to form. For these tests, a current density of 346 amp./sq. ft. (37.4 amp./sq. dm.) was used.

At the higher current densities, higher current efficiencies were obtained: 20.4 per cent at a current density of 48.1 amp./sq. ft. (5.19 amp./sq. dm.) and 63.7 per cent at a current density of 346 amp./sq. ft. (37.4 amp./sq. dm.).

Investigating the effect of different materials on current efficiencies led to the use of a technical grade of trisodium phosphate ($Na_3PO_4 \cdot 12H_2O$). At this point, it was observed that at 340 amp./sq. ft. (35.7 amp./sq. dm.) the efficiency of deposition was increased by increasing the salt content in the bath up to the limit of saturation. The reference bath in the absence of salt gave an efficiency of 52.2 per cent whereas, if 20 grams of the salt were present in the 200 cc. bath, the efficiency was 57.7 per cent. From this point, 200 cc. baths containing the 100 cc. of stock nickel solution and 20 grams of the trisodium phosphate ($Na_3PO_4 \cdot 12H_2O$) were used for the remainder of the preliminary work.

For the bath containing the salt, the current efficiencies were increased by increasing the current densities. Generally speaking, the current efficiencies for this bath over the entire current density range were higher than those obtained for the salt-free bath; being 50.7 per cent at 48.1 amp./sq. ft. (5.19 amp./sq. dm.) and 70.4 per cent at a current density of 346 amq./sq. ft. (37.4 amp./sq. dm.).

With the exception of the trivalent nickel oxide no known compounds of trivalent nickel exist. A solution was prepared using nickelous phosphate ($Ni_3(PO_4)_2 \cdot 7H_2O$) which was identical in all respects with the original stock solution prepared. The equivalent composition of this solution was:

	g./l.	oz./gal.
Nickelous phosphate, $Ni_3(PO_4)_2 \cdot 7H_2O$	74.63	9.93
Phosphoric acid, H_3PO_4(sp. gr. 1.689)	104.4 cc.	0.834 pt.
Trisodium phosphate, $Na_3(PO_4)_2 \cdot 12H_2O$	100	13.33

A comparison of the efficiencies of this solution with an identical solution prepared from nickelic oxide showed that at 340 amp./sq. ft. (35.7 amp./sq. dm.) the baths were for all practical purposes the same.

A sufficient quantity of fresh solution was prepared and divided into two portions for studying the effect of aging. One was used immediately; the second was aged for 96 hours. A comparison of the freshly prepared and the aged solution under identical conditions of operation gave the same plating results.

The stock solution as prepared tended to have a slight amount of suspended material which could not be removed by filtration through paper. A commercial grade of filter aid tended to absorb some of the nickel from the solution. Comparison with an unclarified bath showed that the treatment reduced the current density range and the current efficiency at which good plates were obtainable.

Filtration of a dark green and partly opaque solution through a Buchner funnel having a bed of asbestos fiber (Gooch Crucible Grade) clarified the solution giving one which was completely transparent and light green in color. The filter pad of the asbestos contained a small amount of solids which, when dissolved in aqua regia, showed an absence of nickel and the presence of iron. Measurement of the bath characteristics gave results which indicated that beyond the removal of suspended solids there were no

other observable effects. Solutions that were used beyond this point were clarified in this manner.

To observe the effect of filtration through carbon, a solution containing the trisodium phosphate was treated and filtered through "Norite." On the basis of the loss of color in the first portions of filtrate, a considerable adsorption of the nickel by the carbon had occurred. At a current density of 300 and 400 amp./sq. ft. (27.6 and 36.76 amp./sq. dm. respectively), there was little effect, if any, on the brightness of the plate, but the efficiency was affected in a very detrimental manner.

On the basis of the preliminary work thus far, certain facts became known and were used to guide the research. These are summarized below:

1. Cathode current efficiencies were benefited by higher temperatures.
2. Cathode current densities up to approximately 400 amp./sq. ft. (37.16 amp./sq. dm.) were permissible.
3. The addition of trisodium phosphate gave more favorable results as far as the efficiencies were concerned, but decreased the operating range of the baths.
4. A soluble anode could be used to keep the bath in balance.
5. Filtration of the bath through asbestos could be used for the removal of suspensions.

GENERAL EFFECTS OF PHOSPHATE SALTS ON BATH CHARACTERISTICS

From the preliminary work it was known that trisodium phosphate increased the efficiency of the bath under consideration but narrowed the operating range of the solution. The effect of other phosphates was investigated in order to learn if better addition salts were available.

For this work, the following stock nickel solution was used:

Nickelic oxide, Ni_2O_3	75 g./l.	10 oz./gal.
Phosphoric acid, H_3PO_4 (sp. gr. 1.689)	250 cc./l.	1 qt./gal.

The conditions of use were:

Temperature	85°C.	185°F.
Current density:		
for sodium salts	340 amp./sq. ft.	35.7 amp./sq. dm.
for other salts	190 amp./sq. ft.	20.54 amp./sq. dm.

At the outset, plating was for 18 ampere minutes, but after the runs for the trisodium phosphate were completed, it was decided to run the cells for 5 ampere minutes in order to reduce the time required for operation. A current density other than the one for the sodium salts was used in order to avoid the upper limit of the current density range. Monobasic phosphates (sodium, potassium, and ammonium) were detrimental to the efficiencies, although a considerable tolerance for the salts was evident. The best results were obtained with the tribasic (sodium, potassium) salts.

As a rule, higher efficiencies were observed at the higher salt contents (both dibasic and tribasic) up to the maximum tolerance. However, burning occurred when the nickel content was too low or the salt content was too high. Except in two cases, the optimum results for each salt occurred in a solution where 100 cc. of stock nickel solution were used in a 200 cc. bath. The maximum salt content for the highest efficiencies at this con-

centration of stock nickel solution was, on the basis of 200 cc. of final solution, 20 grams of trisodium phosphate ($Na_3PO_4 \cdot 12H_2O$) (100 g./l., 13.33 oz./gal.), or 25 grams of disodium acid phosphate ($Na_2HPO_4 \cdot 12H_2O$) (125 g./l., 16.66 oz./gal.), 15 g. of diammonium acid phosphate ($(NH_4)_2HPO_4$) (75 g./l., 10 oz./gal.), 12.5 grams of tripotassium phosphate (K_3PO_4) (62.5 g./l., 8.33 oz./gal.), 20 grams of dipotassium acid phosphate (K_2HPO_4) (100 g./l., 13.33 oz./gal.), or 25 grams of microcosmic salt ($NaNH_4HPO_4 \cdot 4H_2O$) (125 g./l., 16.33 oz./gal.). The nickel and acid content corresponding to the above salt contents was:

Nickelic oxide, Ni_2O_3	37.5 g./l.	5 oz./gal.
Phosphoric acid, H_3PO_4 (sp. gr. 1.689)	125 cc./l.	1 pt./gal.

BATH CHARACTERISTICS UNDER OPTIMUM CONDITIONS OF STOCK NICKEL SOLUTION AND SALT CONTENT

On the basis of the conclusions in the preceding section, the range of useable current densities and temperatures was determined for baths of the above-specified optimum compositions. In addition, data for the purpose of comparison were also obtained for two other baths, one of which was salt free, the other containing 4 cc. of ammonium hydroxide (NH_4OH, sp. gr. 0.8980) in a 200-cc. bath (20 cc./l., 0.16 pints/gal.) in place of the phosphate salts. A comparison of the average cathode and anode efficiencies was also made.

The current efficiency and plate characteristics, as a function of temperature and current density as they were measured for the salt free bath, are given in Fig. 1. A 200-cc. bath was used containing 100 cc. of stock nickel solution.

The characteristics of a 200-cc. bath which contained 100 cc. of stock nickel solution and the optimum quantities of phosphate salts are also given in Fig. 1.

The solution which contained only nickel oxide and acid had the greatest operating range, while that containing ammonium hydroxide was next. The solution with the highest efficiencies contained trisodium phosphate. As a rule, there were no limitations with respect to the minimum required current density, except for the cases of disodium acid phosphate and the ammonium hydroxide. From the point of view of efficiencies and conductivity, trisodium phosphate gave the best results as an addition salt. In cases where range was the determining factor, a bath could be used without addition salt whatsoever, even though the voltage required would be 50 per cent higher.

BATH CHARACTERISTICS OF THE SYSTEM NICKELIC OXIDE, PHOSPHORIC ACID, TRISODIUM PHOSPHATE

In accordance with the research concluded, trisodium phosphate was used for the subsequent work. The characteristics of the electrolyte were determined at different concentrations of the stock nickel solution and various quantities of the salt present. For a dilution of 25 cc. of stock nickel solution in a 200-cc. bath, the characteristics are presented in Fig. 2, A-1. The addition of any salt caused a precipitate. The data for other concentrations of constituents are also given in Fig. 2.

A study of the data showed that, at higher nickel-phosphoric acid con-

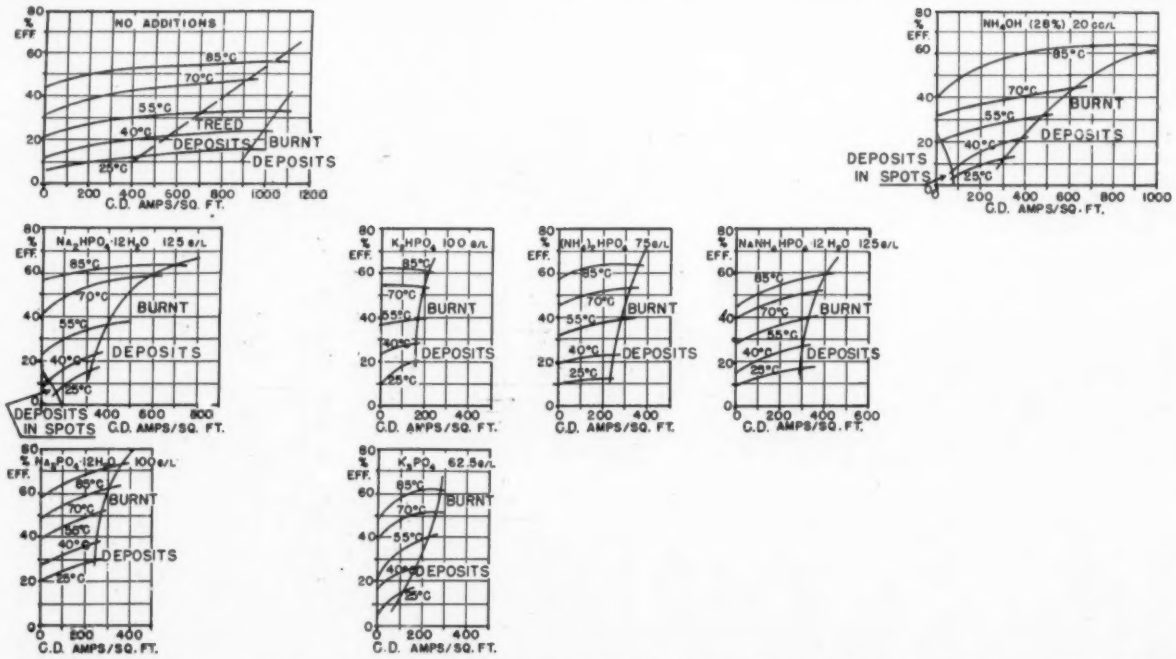

FIG. 1. The bath characteristics of phosphate baths containing 37.5 g./l. Ni_2O_3, 125 cc./l. H_3PO_4 (sp. gr. 1.689) and the indicated optimum quantities of addition salts.

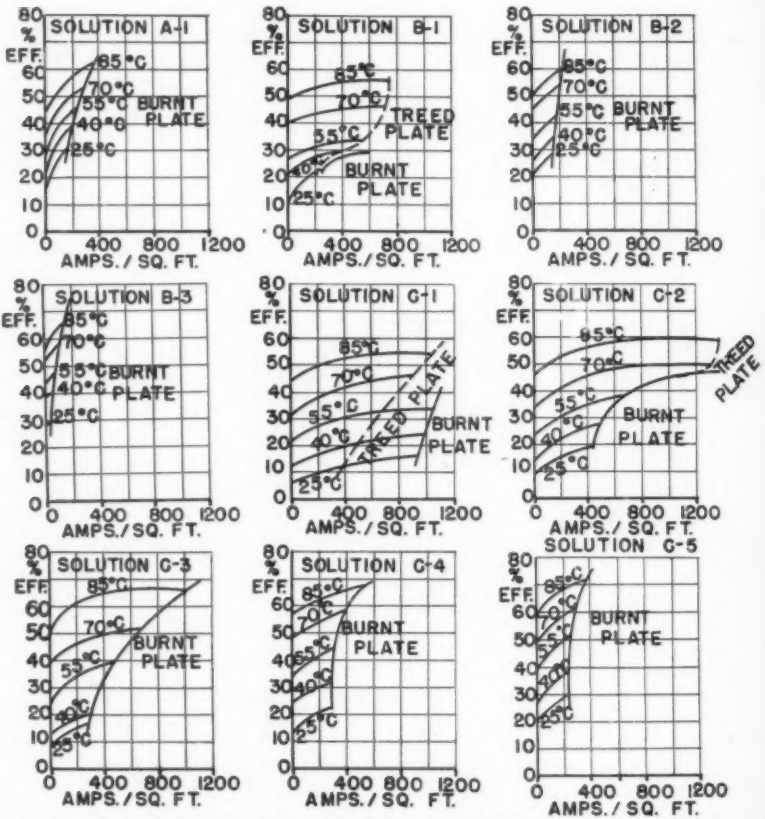

COMPOSITION OF SOLUTIONS USED
(85%) H_3PO_4 IN CC/L Ni_2O_3 & $Na_3PO_4 12H_2O$ IN G/L

	Ni_2O_3	H_3PO_4	$Na_3PO_4 \cdot 12\ H_2O$ -1	-2	-3	-4	-5
A SOLUTIONS	9.375	31.25	0				
B SOLUTIONS	18.75	62.5	0	25	50		
C SOLUTIONS	37.5	125	0	25	50	75	100
D SOLUTIONS	56.25	187.5	0	50	100	150	
E SOLUTIONS	75	250	0	50	100	150	200

FIG. 2. Current efficiency vs. current density vs. plate character at a given composition and temperature.

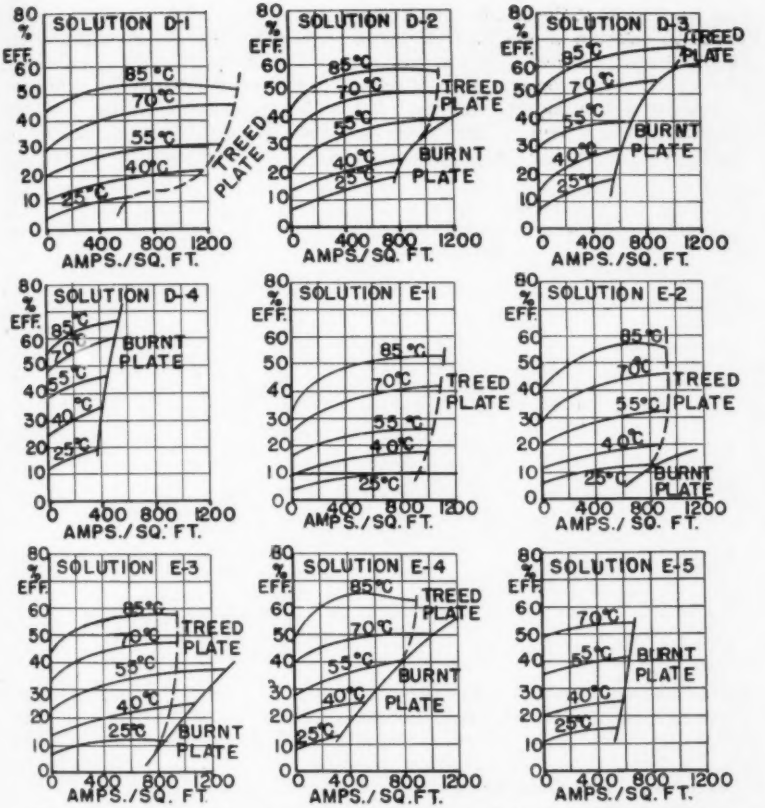

FIG. 2a. Current efficiency vs. current density vs. plate character at a given composition and temperature.

tents, the solution gave broader plating ranges but lower current efficiencies. The addition of salts to the bath increased the current efficiencies but decreased the plating ranges. The bath with the optimum efficiencies contained 100 cc. of stock nickel solution and 20 grams of trisodium phosphate, ($Na_3PO_4 \cdot 12H_2O$), in 200 cc., and the graph is presented in Fig. 2, C-5. The solution with the optimum operating range contained 150 cc. of the stock nickel solution in a 200-cc. bath and is presented in Fig. 2, D-1.

A study of the average cathode and anode efficiency showed the optimum temperature for both processes was 85°C. (185°F.). A summary of the important data at this temperature is presented in Table I. The point at which a maintained bath balance for the various nickel contents is accomplished can be estimated from this table. Such a balance is obtained where the anode efficiency equals the cathode efficiency. It should be

kept in mind that the anode current densities are very high when the area of anode to cathode is one to one. This leads naturally to excessive anode polarization. However, this can be reduced by increasing the anode area, which results in a lower anode current density and decreases the tendency to polarize at the higher currents. If a bath composition to the left of the balance points shown in the table was used, it could be maintained by decreasing the anode area, and consequently increasing the current density.

TABLE I. *Comparison of average cathode (upper figure) and anode (lower figure in parenthesis) efficiency as a function of salt additions and stock nickel content in a 200-cc. bath at 85°C. (185°F.)*

Stock nickel per 200 cc.	Salt ($Na_2PO_4 \cdot 12H_2O$) content in grams per 200 cc.						
	0	5	10	15	20	30	40
cc.							
25	67.1 (80.9)						
50	54.4 (77.5)	59.8 (80.7)	67.8 (59.8)				
100	48.4 (77.0)	52.9 (78.4)	60.4 (46.8)	63.3 (58.9)	67.9 (62.2)		
150	48.1 (88.4)		54.1 (56.0)		60.4 (53.2)	63.5 (57.7)	
200	45.8 (68.7)		49.8 (62.9)		53.8 (57.6)	50.2 (55.1)	44.5 (43.8)

A balance point did not exist in the table for the solution which contained 25 cc. of stock nickel solution in the 200-cc. bath. The only way to maintain a balanced bath was to decrease the anode current density. The balance points for a 200-cc. bath containing:

50 cc. of stock nickel solution was 5 grams of the salt.
100 cc. of stock nickel solution was 10 grams of the salt.
150 cc. of stock nickel solution was 15 grams of the salt.
200 cc. of stock nickel solution was 25 grams of the salt.

STUDIES OF BRIGHTENERS

The possibility of brightening the deposits was of considerable importance since the production of bright deposits directly from the bath would reduce buffing and polishing costs. Thin deposits were bright when taken from the bath. As the thickness of the plate increased, the dullness increased. The plates could be polished by mechanical methods without any trouble.

There are numerous literature references on bright nickel plating. From among those in existence, several were used as guides (8, 9, 10, 11). In addition to the above, the following general brighteners were used: caffeine, glue, licorice root, resorcinol, turkey red oil, gum tragacanth, and dextrose. The above efforts were of no avail. The presence of organic materials, especially of a colloidal nature, tended to be more of a detriment

than an asset. In a few cases, a small amount of grain refinement was produced, but, generally speaking, the effects were negligible.

CONCLUDING WORK

In order to obtain a more complete picture of the phosphate bath, the effect of varying the acid concentration was further studied. A trisodium phosphate salt content was maintained at the maximum tolerance from the point of view of efficiencies. As mentioned in a previous section, if the total phosphoric acid (sp. gr. 1.689) in a liter bath containing 500 cc. of stock nickel solution was increased to 208.4 cc. or to 175 cc. the tolerance for the trisodium phosphate ($Na_3PO_4 \cdot 12H_2O$) became 200 grams or 185 grams respectively. The bath characteristics at 85°C. (185°F.) for this bath are given in Fig. 3.

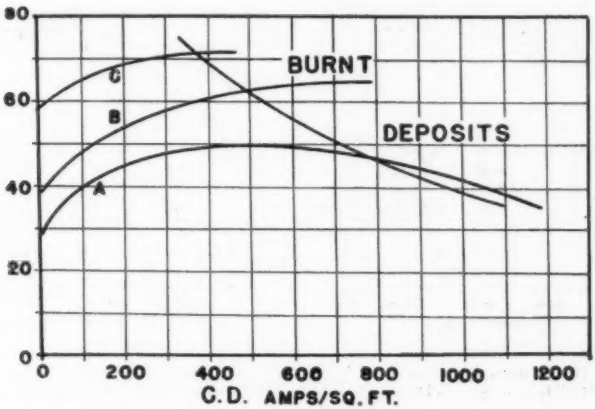

FIG. 3. Bath characteristics at 85°C. (185°F.) of:

$Na_3PO_4 \cdot 12\ H_2O$ g./l.	Ni_2O_3 g./l.	H_3PO_4 (sp. gr. 1.689) cc./l.	Bath
200	37.5	208.4	A
185	37.5	175	B
100	37.5	125	C

If a liter bath was prepared containing 500 cc. of stock nickel solution and (A) 10 grams or (B) 20 grams of sodium hydroxide (NaOH) were added, the tolerance for the trisodium phosphate ($Na_3PO_4 \cdot 12H_2O$) was (A) 50 grams and (B) zero grams respectively. The bath characteristics at 85°C. (185°F.) are shown in Fig. 4.

Examination of this data shows that the addition of acid or base produced a change in both the efficiencies and the ranges, the extent of the increase being dependent on the amount of the addition. The range was even extended beyond the limits given by the salt-free bath, in the case of phosphoric acid addition, whereas the extent was only slightly beyond the salt-free range in the case of sodium hydroxide. On the other hand, the acid addition reduced the efficiencies below, and the addition of the sodium hydroxide increased the efficiencies slightly above the optimum values.

The effect of agitation on the efficiency was investigated using a glass stirrer containing two paddles, each of which was one inch long and 0.5 inch wide (2.54 x 1.27 cm.) and placed at an angle of 30 degrees to the horizontal. It was rotated at 485 RPM in a bath of 600 cc. The bath characteristics as given in Fig. 5 were determined at 85°C. (185°F.). The data showed that the agitation decreased the efficiencies over the entire current range whereas the operating range was slightly increased.

Solutions of this type would not be very important unless they compared with commercial baths. One of the important factors used for such a comparison was the throwing power or the throwing efficiency of a bath, since these show the ability of a given solution to cover an irregularly shaped object. A number of solutions recommended for commercial use were given by Hartshorn (12) and are shown in Table II, which also gives the

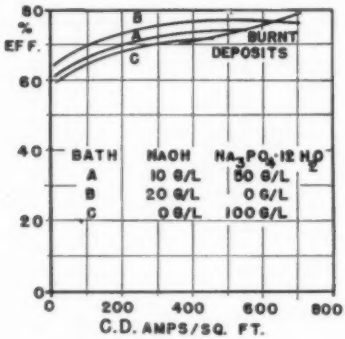

FIG. 4

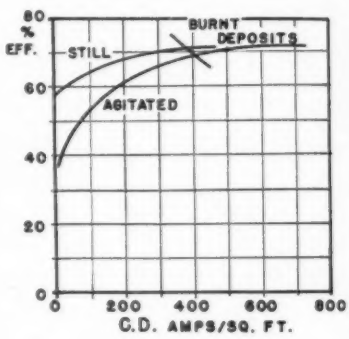

FIG. 5

FIG. 4. Bath characteristics at 85°C. (185°F.) of baths containing 37.5 g./l. Ni_2O_3, 125 cc./l. H_3PO_4 (sp. gr. 1.689) and the indicated quantities of NaOH and $Na_3PO_4 \cdot 12H_2O$.

FIG. 5. Effect of agitation on bath characteristics at 85°C. (185°F.) of a bath containing 37.5 g./l. Ni_2O_3, 125 cc./l. H_3PO_4 (sp. gr. 1.689) and 100 g./l. $Na_3PO_4 \cdot 12H_2O$.

throwing power and throwing efficiency in comparison with the phosphate solutions. In these measurements, the cell was 5.75 inches long, 1.75 inches wide, and 2 inches high (14.6 x 4.45 x 5.08 cm.). When filled with 250 cc. of electrolyte, the depth was approximately 1.75 inches (4.45 cm.). The introduction of a soluble nickel anode and the two copper cathodes formed a system wherein the far cathode was 115 mm. (4.52 in.) from the anode and the near cathode was 21 mm. (0.827 in.) from the anode. The primary distance ratio was thus 5.48.

For the first run in Table II, 0.1974 gram was deposited on the near cathode and 0.0521 gram was deposited on the far cathode, giving a metal distribution ratio of 3.77. Thus, the throwing power was equal to 31.2 per cent, and the throwing efficiency was equal to 38.2 per cent. The throwing efficiency of the phosphate bath at the recommended operating temperatures (85°C., 185°F.) is 29.7 per cent. The throwing efficiency of the sulfate baths are 35.5 per cent for the dilute one and 38.9 per cent for

the more concentrated one, whereas that of the chloride bath is 38.2 per cent. These figures indicate that the throwing efficiencies of the phosphate bath are not far out of line.

The economic aspects of the electrolyte were of considerable importance. Comparison of the voltages measured in the throwing power tests showed that the energy consumption of the phosphate process for a given weight of metal would be about 5 times as high as the sulfate baths. Considering

TABLE II. *Comparison of the throwing power (T. P.) and efficiency (T. E.) of commercial and phosphate baths*

Solution A	Solution B	Solution C	Solution D (C-5)
Compositions of baths used in g./l. or cc./l.			
$NiSO_4 \cdot 6H_2O$..... 120	$NiSO_4 \cdot 6H_2O$.... 180	$NiCl_2 \cdot H_2O$ 300	Ni_2O_3..... 37.5
NH_4Cl..... 22.5	NH_4Cl..... 24.75	Boric acid..... 30	H_3PO_4 (sp. gr. 1.689)..... 125
Boric acid..... 30	Boric acid..... 30		$Na_3PO_4 \cdot 12H_2O$..... 100
Operating conditions			
Temp.....75–85°F.	Temp.....120–140°F.	Temp.....140°F.	Temp.....185°F.
C. D.....5–15 amp./ft.^{2}	C. D....25–50 amp./ft.^{2}	C. D..100 amp./ft.^{2}	C. D.....300 amp./ft.^{2}
pH.....5.4–6.0	pH.....5.6–5.9	pH.....2.0	pH.....2.0

Anode area is 5.49 in.^{2} Cell distance ratio (D. R.) is 5.48.

Sol'n.	Dep. on cathode		M. D. R.	Time	Temp.	Amp.	Volts	Cathode area	C. D.	T. P.	T. E.
	Near	Far									
	g.	*g.*		*min.*	°F.			*sq. in.*	*amp./ sq. ft.*	%	%
A	0.1974	0.0527	3.77	60	75	0.25	1.7	2.572	14	31.2	38.2
B	0.3385	0.0869	3.89	30	138	0.9	1.9	2.624	49.5	28.0	35.5
B	0.3433	0.0833	4.09	40	77	0.7	2.9	2.576	39.1	25.3	31.0
C	0.5489	0.1469	3.73	30	137	1.5	1.9	2.672	80.8	31.7	38.9
C	0.5701	0.1289	4.42	30	72	1.5	2.7	2.622	82.4	19.3	23.7
D	0.5821	0.1298	4.48	10	185	5.0	8.4	2.624	274	18.22	22.3
Because of the large amount of anode corrosion some of the disintegrated anode was occluded in the deposit so that for the phosphate bath anode bags were used.											
D	0.4466	0.1077	4.15	10	185	4.0	8.1	2.532	228	24.3	29.7
D	0.2105	0.0331	6.33	15	77	3.0	10.4	2.552	169.2	−15.5	−18.9

the point that the energy costs were of a secondary nature in an electroplating plant and that the costs of equipment, electrolyte, and space occupied were of a primary importance, the problem of the increased energy costs is not a serious objection.

Another important economic aspect is the costs of the electrolyte. An estimate of the unit costs of the four solutions represented in the Table II on a basis of reported market (13) prices showed that the cost of the materials required would be: 3.65 cents per liter for the phosphate bath, 3.90 cents per liter for the 120-gram sulfate bath, 5.81 cents per liter for the

180-gram sulphate bath, and 14.81 cents per liter for the chloride bath. Even at higher quoted prices (13) the costs for the largest lots would be 44.25 cents per liter for the phosphate bath, 14.81 cents per liter for the 120-gram sulphate bath, 21.22 cents per liter for the 180-gram sulphate bath, and 124.4 cents per liter for the chloride bath. Considering that the total quantity of the electrolyte required was less because of the higher current density, the capital investment required would be smaller. The simple analysis shown herein indicated that the phosphate bath compared favorably with the nickel plating solutions commercially in use at the present time.

SUMMARY

1. Nickel plates were obtained from a phosphate bath over a considerable range of current densities, temperatures, and compositions. The optimum efficiency was obtained using a solution which contained:

	g./l.	oz./gal.
Nickelic oxide, Ni_2O_3	37.5	5.0
Phosphoric acid, H_3PO_4(sp. gr. 1.689)	125 cc.	1 pint
Trisodium phosphate, $Na_3PO_4 \cdot 12H_2O$	100	13.33

Operating conditions:

Temperature	85°C.	185°F.
Current density	340 amp./sq. ft.	36.7 amp./sq. dm.

2. The composition of the electrolyte for the optimum operating range was:

	g./l.	oz./gal.
Nickelic oxide, Ni_2O_3	56.25	7.5
Phosphoric acid, H_3PO_4(sp. gr. 1.689)	187.5 cc.	1.5 pints

Operating conditions:

Temperature	85°C.	185°F.
Current density	1200 amp./sq. ft.	130 amp./sq. dm.

3. Balance can be maintained in the bath by the use of soluble anodes, and the proper ratio of the anode area to cathode area.

4. The electrolyte can be prepared by the dissolution of nickelic oxide, Ni_2O_3, in phosphoric acid (sp. gr. 1.379) at 105°C. (221°F.). Other methods of preparation can be used if the final composition is identical with the desired solution.

5. The addition of dibasic and tribasic phosphates up to the limits of saturation (providing burning did not occur) to the solution prepared in 4 increased the current efficiency. Of all of the phosphate salts, the trisodium phosphate gave the best results.

6. The presence of acid in greater concentrations than specified above gave baths which had greater plating ranges than the solution given in 1 but the efficiencies were generally lower.

7. The addition of sodium hydroxide to reduce the free acid concentration produced baths with greater plating ranges than that obtainable in 1. The efficiencies obtainable generally were slightly higher than the efficiencies obtainable from the solution given in 1.

8. Agitation of the electrolyte produced a slightly broader operating range and lower efficiencies than those obtainable from a still bath.

9. Additions of the normal brighteners produced detrimental results with the exception of a few cases where a slight grain refinement was produced. It was possible to produce bright deposits mechanically by buffing the plates using standard commercial buffing sticks.

10. The throwing power of the phosphate bath compared favorably with that of the commercial sulfate and chloride baths in use. The phosphate bath operated under conditions given in part 1 of this section gave a throwing efficiency of 29.7 per cent. The more dilute sulfate bath operated under its optimum conditions gave a throwing efficiency of 35.5 per cent. The current efficiencies of the phosphate bath were lower than those obtainable from a sulphate-chloride bath.

11. The economic aspects of the utilization of the phosphate bath commercially were favorable.

Any discussion of this paper will appear in the discussion section of Volume 94 of the Transactions of the Society.

REFERENCES

1. Maigne and Mathey, "Manuel de Dodure," p. 333 (1891 ed.).
2. S. Koyonagi, *Bull. Chem. Soc. Japan*, **10**, 255–6, 355–6 (1935).
3. G. Langbein and W. Brannt, "Electroplating," p. 319 (1909 ed.).
4. J. Powell, U. S. Pat. 228,389, June 1, 1880.
5. ————, U. S. Pat. 229,274, June 29, 1880.
6. G. Langbein, "Electroplating," p. 318 for nickel.
7. A. Levy, U. S. Pat. 923,864, June 8, 1909.
8. L. Weisberg and W. B. Stoddard, U. S. Pat. 2,026,718, Jan. 7, 1936.
9. M. Schlotter, U. S. Pat. 1,972,693, Sept. 4, 1934.
10. V. H. Waite, U. S. Pat. 2,112,818, Mar. 29, 1938 and 2,114,006, Apr. 12, 1938.
11. R. Lind and W. J. Harshaw, U. S. Pat. 2,198,267 and 2,198,268, Apr. 23, 1940.
12. D. S. Hartshorn, "Plating and Finishing Guide Book" (1946).
13. *Oil, Paint Drug Reptr.*, Jan 13, (1947).